

UNIVERSITY OF BELGRADE

SCHOOL OF MEDICINE

Đurđa N. Bracanović

RADIOLOGICAL AND
IMMUNOHISTOCHEMICAL ANALYSES
OF HYPEROSTOSIS FRONTALIS
INTERNA: MULTI-LEVEL APPROACH TO
UNDERSTANDING THE DEVELOPMENT
OF THIS PHENOMENON

Doctoral Dissertation

Belgrade, 2016

УНИВЕРЗИТЕТ У БЕОГРАДУ
МЕДИЦИНСКИ ФАКУЛТЕТ

Ђурђа Н. Брацановић

РАДИОЛОШКА И
ИМУНОХИСТОХЕМИЈСКА АНАЛИЗА
ХИПЕРОСТОЗЕ ФРОНТАЛНЕ КОСТИ:
МУЛТИДИСЦИПЛИНАРАН ПРИСТУП У
РАСВЕТЉАВАЊУ НАСТАНКА ОВОГ
ФЕНОМЕНА

докторска дисертација

Београд, 2016

PhD advisor:

Associate professor dr Danijela Đonić
University of Belgrade – School of Medicine

Members of the evaluation committee:

1. Professor dr Marija Đurić, University of Belgrade – School of Medicine
2. Professor dr Zoran Rakočević, University of Belgrade – School of Dental
Medicine
3. Professor dr Jelena Sopta, University of Belgrade – School of Medicine
4. Associate professor dr Vladimir Živković, University of Belgrade – School of
Medicine
5. Professor dr Dragana Bogdanović, University of Novi Sad - School of Medicine

Date of public presentation: _____

This way, I would like to express my gratitude to those who contributed, both directly and indirectly, to this PhD thesis.

First, I would like to express my sincere gratitude to my PhD advisor, associate professor Danijela Djonic, for her continuous guidance, time and effort invested in every segment of this PhD thesis. I really appreciate her support, patience and motivation to help me overcome every obstacle and problem during this research. Above all, I admire her personally, and I am grateful for our collaboration.

I owe special gratitude to my professors, Prof. Marija Djuric and Prof. Zoran Rakocevic, for the help and guidance, both personal and professional, during my PhD studies and professional carrier. Their support contributed my research significantly, but their professionalism and endless energy are something I admire.

I am grateful to the members of the PhD Advisory board for constructive suggestions regarding this thesis.

I am thankful to Prof. Slobodan Nikolic and associate professor Vladimir Zivkovic, for given opportunity to collaborate with them during this PhD research and wide support they have provided.

I would like to thank Dr. Miomira Iovic for conducting densitometric evaluation in our research and Dr. Katarina Rajkovic for performing fractal analysis of the radiographs used in our study. I owe gratitude to Prof. Jelena Sopta and Dr. Relja Kovacevic, for performing immunohistochemical analysis of the dura samples. I would like to thank my dear colleagues and friends: Dr. Petar Milovanovic for helping me in micro-CT analysis of frontal bone samples, Dr. Aleksa Janovic for helping me process images for the thesis and Ksenija Djukic for all the help during our PhD studies.

I would like to thank my colleagues from the Laboratory for Anthropology for their help and support.

Finally, I would like to express my deepest gratitude to my family, for believing in me all these years. Thank you for your love and support.

Title of the doctoral dissertation:

RADIOLOGICAL AND IMMUNOHISTOCHEMICAL ANALYSES OF HYPEROSTOSIS FRONTALIS INTERNA: MULTI-LEVEL APPROACH TO UNDERSTANDING THE DEVELOPMENT OF THIS PHENOMENON.

Summary

Background

Hyperostosis frontalis interna (HFI) is the overgrowth of bony tissue on the inner plate of the frontal bone. Females manifest significantly higher prevalence of HFI compared to males, with the peak incidence in postmenopausal women. Etiopathogenesis of HFI is still ambiguous. Different hormonal imbalances i.e. prolonged estrogen stimulation during reproductive period, or abnormal progesterone effect on the ovaries, or inadequate androgen stimulation are pointed out in the literature as the most probable causes of HFI, due to its high prevalence and severity in the females, as well as the fact that in males only those with hypogonadism manifest advanced stages of HFI. Several models have tried to provide an adequate explanation of HFI development. The most recent is the „global model“ which states that neovascularization originating from dura, might be one of the key processes in its formation. Some studies suggested that women with HFI tend to develop more robust skull characteristics. However, there are no studies that investigated whether HFI is accompanied by changes in bone thickness or density in postcranial skeleton. Present macroscopical classification of HFI is based on morphological characteristics and extension of frontal bone involvement and includes four different types of HFI. Relatively low percentage of radiological recordings of HFI may occur due to the fact that present macroscopical method of identification and classification encompasses multiplanar reconstruction of head CT scans, which makes it complicated for routine radiological practice. Additionally, it remains unclear whether different macroscopic stages of HFI can be regarded as successive phases in the process of HFI development.

Hypothesis

The frontal bone thickening in women with HFI is accompanied by increased bone thickness of the entire skull

The frontal bone thickening in women with HFI is accompanied by increased bone thickness and increased bone density in the postcranial skeleton

Frontal bone is particularly affected by HFI due to specific properties of its underlying dura

Morphological appearance of different types of HFI defined in macroscopic classification are accompanied by corresponding differences in internal bone architecture

It is possible to simplify current classification of HFI for radiological practice

Material and methods

This study comprised four research phases. The first phase was designed as a cross-sectional study. It was conducted in the Center for Radiological Diagnostics of School of Dental Medicine, University of Belgrade. Study sample included 103 women who underwent computerized tomography (CT) of the head, done for diagnosis of chronic sinusitis. Only postmenopausal women (women who had their final menstrual period at least 12 months prior) with confirmed diagnosis of chronic sinusitis and who performed head CT scan for the first time were eligible to participate in this study. Exclusion criteria were presence of bone related pathologies other than HFI, as well as medical history of brain tumor, meningioma, renal diseases, primary hyperparathyroidism and Paget's disease. Based on the head CT scan analyses results, women were categorized in the control group (without HFI) and the group with HFI. The correlation between the presence of HFI and thickness of other cranial bones was assessed on head CT scans, by measuring cranial bones thickness while dual energy x-ray absorptiometry was used to determine possible changes in bone density between two investigated groups. Additionally, external geometry of the proximal femur between

women with HFI and control group was analyzed using hip structure analysis. For the purpose of sample collection for the second and third research phase, frontal bone samples and samples of its underlying dura, were collected during routine autopsies from human donor cadavers at the Institute of Forensic Medicine of the School of Medicine in Belgrade. The second phase of our study comprised immunohistochemical analyses of α -estrogen and CD34 receptors on dura underlying frontal bone, collected from 12 women with HFI and an age-matched control group of 15 women. Modified „Chalkley“ count method was utilized to measure microvessel density. The third phase included assessment of the 3D-microarchitecture of the frontal bone in 20 women with various types of HFI and 14 women in age-matched control group. The study sample in the fourth research phase comprised 73 women with various types of HFI and included fractal analysis of their head computerized tomography (CT) scans. By comparing the values of the parameters of shape (fractal dimension and circularity) we compared different types of HFI.

Results and conclusion

Apart from a thicker frontal bone compared to women without HFI, women with HFI had thicker occipital and parietal bones as well. Additionally, our results suggested that frontal bone is the first one to thicken, followed by parietal and occipital bones respectively. In women with HFI, values of densitometric parameters in the spine and hip region did not significantly differ when compared to the age-matched post-menopausal control group. Results of external geometry of the proximal femur analysis also did not indicate any significant differences between investigated groups of women. 3D-microarchitectural analysis of the frontal bone in women with HFI and in an age- and sex-matched control group revealed that the women with HFI showed significantly higher bone volume fraction in the region of diploe, along with significantly thicker and more plate-like shaped trabeculae and reduced trabecular separation and connectivity density. Moreover, inner table of the frontal bone in women with HFI displayed significantly increased total porosity and mean pore diameter compared to controls. Therefore, it is possible that larger pores occur as a result of penetration of blood vessels from the dura, ultimately leading to diploization of the inner table. Analysis of the

expression of CD34 receptors on the dura of the frontal region in women with HFI and the control group clearly showed that in women with HFI expression of CD34 was significantly increased, thus the vascularization was increased. Method of fractal analysis of the head CT scans of women with HFI detected significant differences of parameters of shape only between type D of HFI in comparison to types A, B and C of HFI.

The results of our study demonstrated that increased bone thickness and altered bone structure in women with HFI are localized only on the skull, particularly on the frontal bone and indicated that in the postcranial skeleton bone density did not differ between women with and without HFI. If sex steroid hormone disbalance participates in the pathogenesis of HFI, it could be by inducing only the local changes in dura and therefore resulting in increased vascular formation and osteoblast proliferation on the skull. Increased vascularization of the dura underlying frontal bone in women with HFI clearly implies the correlation between the expanded blood supply, of any origin, and HFI formation. Macroscopic types of HFI could not be distinguished at the level of bone microarchitecture and their consecutive nature cannot be supported. Rather, our study suggests that only two different types of HFI (moderate and severe HFI) have microstructural and justification by the method of fractal analysis, and should be further considered.

Keywords: *Hyperostosis; frontal bone; osteoporosis; postmenopausal women; micro-architecture; dura.*

Scientific field: Medicine

Specific scientific field: Skeletal biology

Наслов докторске дисертације:

РАДИОЛОШКА И ИМУНОХИСТОХЕМИЈСКА АНАЛИЗА ХИПЕРОСТОЗЕ ФРОНТАЛНЕ КОСТИ: МУЛТИДИСЦИПЛИНАРАН ПРИСТУП У РАСВЕТЉАВАЊУ НАСТАНКА ОВОГ ФЕНОМЕНА.

Резиме

Увод

Hyperostosis frontalis interna (HFI tj. ХФИ), представља нагомилавање коштаног ткива локализовано на унутрашњој површини фронталне кости. Чешће се јавља код особа женског пола са највишом инциденцом забележеном код жена у постменопаузи. Етиопатогенеза ХФИ и даље није разјашњена. Различити хормонски дисбаланси као што је пролонгирана естрогена стимулација током репродуктивног периода, поремећена продукција прогестерона од стране оваријума или неадекватна андоргена стимулација су у литератури наведени као највероватнији узрочници настанка ХФИ, имајући у виду високу преваленцу и израженију манифестацију ХФИ код жена, као и чињеницу да се само код мушкараца са хипогонадизмом јављају изражене форме ХФИ. Неколико модела је понуђено као могуће објашњење процеса настанка ХФИ. Најновији је “глобални модел“, по коме неоваскуларизација, пореклом из дуре, може бити један од кључних процеса у настанку ХФИ. У појединим студијама примећено је да жене са ХФИ могу развити робусније морфолошке карактеристике лобање у односу на оне без ХФИ. Међутим, не постоје студије које су испитивале да ли је ХФИ праћена променама у коштаном густини и спољашњој морфологији и у посткранијалном делу скелета. Постојећа макроскопска класификација ХФИ је базирана на морфолошким карактеристикама и обиму захваћености фронталне кости и обухвата четири различита типа ХФИ (А, Б, Ц и Д). Релативно низак проценат бележења ХФИ од стране радиолога, може се објаснити чињеницом да постојећи макроскопски метод класификације и идентификације ХФИ обухвата тродимензионалну реконструкцију прегледа главе начинјених методом компјутеризоване томографије (СТ), и да је као такав, сувише компликован за

рутинску радиолошку праксу. Такође, и даље није познато да ли различити макроскопски типови ХФИ могу бити посматрани као сукцесивне фазе у процесу настанка ХФИ.

Хипотезе

Код жена са ХФИ, поред задебљале фронталне кости, задебљале су и остале кости лобање.

Задебљање фронталне кости код жена са ХФИ, праћено је повећањем коштане густине и дебљине и на посткранијалном делу скелета.

ХФИ захвата фронталну кост због специфичних особина дуре која на њу належе.

Морфолошки изглед различитих типова ХФИ, дефинисаних на основу макроскопске класификације, праћен је одговарајућим разликама у унутрашњој архитектури фронталне кости.

Могуће је упростити актуелну класификацију ХФИ за употребу у радиолошкој пракси.

Материјал и методе

Ова студија се стастојала од четири истраживачке фазе. Прва фаза је дизајнирана као студија пресека. Спроведена је у Центру за радиолошку дијагностику, Стоматолошког факултета, Универзитета у Београду. Испитивани узорак чиниле су 103 жене, које су обавиле радиографисање главе методом СТ, због хроничног синуситиса. Само жене у постменопаузи (жене које су последњи менструални циклус имале најмање 12 месеци пре радиографисања), са потврђеном дијагнозом хроничног синуситиса и које преглед главе СТ методом раде по први пут, укључили смо у студију. Из студије смо искључили све жене са обољењима костију (осим ХФИ), туморима мозга, менингеомима, бубрежним обољењима, примарним хиперпаратиреозом и Паџетовом болешћу. На основу резултата прегледа главе методом СТ, испитивани узорак поделили смо у

контролну групу (жене које немају ХФИ) и групу жена са ХФИ. Могућу корелацију између постојања ХФИ и дебљине кранијалних костију испитивали смо на СТ радиограмима главе, тако што смо мерили дебљину фронталне, паријеталних и окципиталне кости. Како би смо испитали могуће разлике у коштаног густини на посткранијалном делу скелета, између испитиваних група жена, користили смо двоенергетску рендгенску апсорпциометрију (*DXA*). Разлике у спољашњој геометрији проксималног фемура између жена са ХФИ и жена у контролној групи испитиване су структурном анализом кука (*HSA*).

У циљу прикупљања узорака за другу и трећу фазу истраживања, узорци фронталне кости и дуре која на њу належе, сакупљени су са кадавера донора, током рутинских обдукција на Институту за судску медицину, Медицинског факултета, Универзитета у Београду. Друга фаза истраживања обухватила је имунохистохемијску анализу α -естрогенских и CD34 рецептора на дури која належе на унутрашњу површину фронталне кости, сакупљену од 12 жена са ХФИ и 15 истодобних жена у контролној групи. Модификовани „*Chalkey*“ метод бројања је коришћен како би се испитала густина крвних судова на дури квантификацијом експресије CD34 рецептора. Трећа фаза истраживања обухватила је процену тродимензионалне микроархитектуре фронталне кости код 20 жена са различитим типовима ХФИ и код 14 истодобних жена у контролној групи. У четвртој фази истраживања испитивани узорак чиниле су 73 жене са различитим типовима ХФИ. Њихови СТ радиограми главе анализирани су методом фракталне анализе. Поредећи вредности параметара облика добијених методом фракталне анализе, поредили смо различите типове ХФИ.

Резултати и закључак

У односу на контролну групу, жене са ХФИ имале су осим дебље фронталне кости, и дебље паријеталне и окципиталну кост. Наши резултати су такође указали да фронтална кост прва задебљава, а затим сукцесивно паријеталне па окципитална кост. Вредности денситометријских параметара у регионима кука и кичме, нису се сигнификантно разликовали када смо поредили жене са ХФИ и контролну групу. Резултати анализе спољашње геометрије проксималног фемура такође нису указали на постојање сигнификантних разлика између испитиваних

група жена. Троструктурна микроструктурна анализа фронталне кости жена са ХФИ и истодобне контролне групе жена, показала је значајне разлике. Жене са ХФИ имале су значајно виши проценат коштане фракције у регији диплое, значајно дебље трабекуле организоване у коштаном ткиву “тањирасте“ структуре, као и значајно мање вредности степена сепарације трабекула и степена повезаности трабекула, у поређењу са женама у контролној групи. Шта више, структура унутрашње ламине фронталне кости код жена са ХФИ показала је значајно више вредности тоталне порозности и просечне величине пора у поређењу са контролном групом. Веће поре у унутрашњој ламини фронталне кости жена са ХФИ могу настати као последица пенетрације крвних судова из дуре, доводећи до диплоизације унутрашње ламине. Анализа експресије CD34 рецептора на дури фронталног региона код жена са ХФИ у поређењу са контролном групом, јасно је показала значајно већу експресију овог рецептора код жена са ХФИ, и указала на повећану васкуларизацију. Метод фракталне анализе радиограма главе жена са различитим типовим ХФИ, показао је значајне разлике у параметрима облика само између ХФИ типа Д, у поређењу са ХФИ типом А, Б и Ц.

Резултати наших истраживања показали су да се код жена са ХФИ повећана дебљина и измењена структура костију јављају само на лобањи, посебно на фронталној кости, док на посткранијалном делу скелета нема разлика између испитиваних група. Уколико дисбаланс полних хормона учествује у настанку ХФИ, свој утицај могао би да оствари индукујући локалне промене само на дури, које доводе до њене повећане васкуларизације и последично повећане пролиферације остеобласта на костима лобање. Повећана васкуларизација дуре која належе на фронталну кост, код жена које имају ХФИ, недвосмислено указује на корелацију између појачане васкуларизације, било ког порекла, и настанка ХФИ. Макроскопски типови ХФИ не разликују се на нивоу коштане микроструктуре, тако да нема доказа који подржавају теорију о њиховој сукцесивној природи. Тачније, наши резултати анализе микроструктуре и фрактална анализа указују на то да само два различита типа ХФИ (умерени и изражени тип) треба разматрати.

Кључне речи: *Хиперостоза; фронтална кост; остеопороза; менопауза; микро-архитектура; дура.*

Научна област: медицина

Ужа научна област: биологија скелета (остеологија)

Table of Contents

1	Introduction	1
1.1	Hyperostosis frontalis interna	1
1.2	Differential diagnosis of HFI	2
1.3	Sex and age distribution of HFI	3
1.4	Etiology of HFI	4
1.5	HFI in historical and modern populations	5
1.6	Frontal bone	7
1.7	HFI in relation to other skeletal sites	8
1.8	Symptoms of HFI	8
1.9	Pathogenesis of HFI	10
2	Research goals	12
3	Material and methods	13
3.1	Clinical study	13
3.1.1	Head CT scans	14
3.1.2	Cranial bones thickness	15
3.1.3	Symptoms and conditions related to HFI	16
3.1.4	DXA scans and HSA analyses	17
3.2	Analyses of α -estrogen and CD34 receptors on dura	19
3.3	Micro structural analysis	20
3.4	Fractal analysis	24
3.4.1	Digital image processing	25
3.4.2	Parameters of shape of the inner contour	26
3.4.3	Fractal dimension of the inner contour	26

3.4.4	Circularity of the inner contour	27
3.5	Statistical analysis.....	28
4	Results	30
4.1	Clinical research	30
4.1.1	Symptoms and conditions related to HFI	30
4.1.2	Cranial bones thickness	30
4.1.3	DXA scans and hip structure analyses	33
4.2	Analyses of α -estrogen and CD34 receptors on dura	38
4.3	Micro structural analysis.....	41
4.4	Fractal analysis	47
5	Discussion	49
6	Conclusions	61
7	References	63

1 Introduction

1.1 Hyperostosis frontalis interna

Hyperostosis frontalis interna (HFI) is the condition firstly described by pathologist Giovanni Batista Morgagni, a Padua University professor of anatomy, as a “specific variety of bone accretion localized on the inner table of the frontal bone” (1). He also observed co-occurrence of HFI with obesity and hirsutism. More than 200 years later, Stewart (2), Morel (3) and Moore (4) described that persons with HFI often suffered from headache and neuropsychiatric disorders and when these conditions were brought to connection with hormonal disorders they altogether formed Morgagni-Stewart-Morel-Moore syndrome (5).

The diverse terminology related to the phenomenon of HFI testifies to the variety of opinion concerning whether HFI is a sole phenomenon or it is related to other conditions that lead to cranial bones thickening such as hyperostosis cranii diffusa (HCD) and hyperostosis calvaria interna (HCI) (4, 6, 7). Moore (4) considered HFI and HCD to be different manifestations of the same process, with HFI occurring first, as a precursor to HCD. Perou (6), on the other hand, offered the term HCI which includes all cases of endostosis, regardless of their endocranial location and he defined it as a “bilateral, dysplastic, slow, often self-limited and benign, occasionally progressive and aggressive, proliferation of bone involving primarily the inner table of the skull, with or without participation of the diploe, and with a predilection for the frontal squama”. He also pointed out the differences between HCI and HCD. Unlike HCI, HCD is primarily a dystrophic and degenerative process, not related to heredity, not influenced by sex or age, without racial predominance and with no specific clinical picture.

Finally, Hershkovitz et al. (7) gave priority to the term HFI over HCI, since HFI is the common term in the medical literature, and due to the fact that involvement of other areas of endocranium may imply different etiology. They defined HFI as the overgrowth of bony tissue on the inner plate of the frontal bone with the presence of single or multiple bony nodules. Some authors reported that HFI is usually restricted to

the area between the superior sagittal sinus and skull midline, while posterior, the ascending branch of the middle meningeal artery serves as a limiting factor.

Based on extent of involvement of the frontal bone, appearance, border type, shape, location in frontal bone and involvement of other bones, Hershkovitz et al. (7) developed a classification method of HFI:

Type A: Isolated, elevated bony island(s), single or multiple, unilateral or bilateral, all of which exhibited discrete, often indented margins. These were generally under 10 mm in size, and were commonly found on the anteromedial part of the frontal bone.

Type B: Nodular bony overgrowths, without discrete margins and with only slight elevation identified on less than 25% of the frontal bone. Occasionally isolated nodular areas were also identified.

Type C: More extensive nodular bony overgrowth, associated with irregular thickening of up to 50% of the frontal endocranial surface. A tendency for greater elevation and coalescence was observed.

Type D: Continuous bony overgrowth, involving more than 50% of the frontal endocranial surface. The entire region was found to be irregularly elevated with sharp, clearly demarcated borders.

1.2 Differential diagnosis of HFI

The differential diagnosis of HFI includes various pathologies: focal masses (i.e., meningioma, endosteal osteoma), subdural and dural calcifications, Paget's disease, acromegaly, and fibrous dysplasia (8). The characteristics of HFI (including clear boundaries along the middle meningeal artery, unaffected midline, and a tendency towards bilaterality) allow us to make clear differentiation of HFI from most of the mentioned processes (7). Unlike HFI, osteomas tend to be localized on the ectocranial surface and they are rarely bilateral (8). Large bony masses such as meningiomas and calcified subdural hematomas do not follow the macroscopical criteria for HFI identification and classification, proposed by Hershkovitz et al. (7). Acromegaly is a

generalized process with an increase in the diploic space and significant thickening of inner and outer tables of all skull components. Fibrous dysplasia is a process of diploic space expansion, associated with the thinning of both inner and outer tables of the skull. Paget's disease involves most of the cranial bones, and shows thickening of both inner and outer tables (7). Facial bone involvement is not recognized in HFI, while it can be present in Paget's disease and fibrous dysplasia (7).

1.3 Sex and age distribution of HFI

Moore (1955) reported that HFI occurs in 5-12% of the general population, while the highest incidence of HFI (40-60%) is reported in postmenopausal women (9). Reported rates of HFI for females and males respectively are 20% and 2% (10), 24% and 5.2% (7), 18% and 0.7% (11), 22.7% and 2.8% (12). These data imply that HFI is relatively uncommon in males (4–5 times less frequent than in females). Additionally, men with HFI usually manifest mild forms of HFI, suggesting that the severity of HFI is also sex dependent (7). When present in men, HFI is usually moderate in extent (usually types A and B according to Hershkovitz's classification), while Type D is rarely reported. Severe cases of HFI were found only in men who suffered from hypogonadism (13, 14). Sex derived discrepancy in frequency and magnitude of manifestation of HFI may occur as a result of different susceptibility to causative factors such as heredity, endocrine disorders, dysplasia, dystrophy, neoplasia and trauma (6).

Apart from the fact that it is rare in young population, initially there was no consent whether HFI is age related. Moore (4) considered that HFI is progressing with advancing age, while Marlet (10) was more forbearing. He stated that HFI is not a typical aging phenomenon, since he detected an increase in the frequency of HFI in women over age of 50 years, but the magnitude of manifestation of HFI did not correlate with age. The result of the study conducted by Nikolic et al. (11) also showed that older the woman was, the higher was the probability of HFI occurrence, but with no correlation to the extent of frontal bone involvement. Marlet (10) speculated that HFI can develop during an 8-year period and then remain silent for the next 6–11 years. Hershkovitz et al. (7) pointed out to the possible "self-limiting" mechanism of HFI,

since their results showed that, in patients aged over 70 years, the frequencies of mild and severe cases of HFI were almost the same. Marlet (10) claimed that “HFI is an irregular process which once started, can show progression but can stabilize or even subside”. Based on a radiological study, Salmi et al. (15) suggested that HFI reaches its peak in age group of 40 to 60 years, and then rapidly diminishes. Finally, HersHKovitz et al. (7) concluded that HFI is an age dependent phenomenon, since it is much less frequent in females under 40 years of age and that advanced cases of HFI are more frequently found after the age of 60 years.

1.4 Etiology of HFI

Etiology of HFI is still unclear. All the presumptions of its etiology are mainly based on alteration of sex steroids and its impact on adult bone growth. Richter (16) was the first to postulate the speculation that female hormonal changes are responsible for HFI formation. Perou (6) stated that hyperostosis “needs a given soil to start and a given stimulus to manifest itself” and suggested endocrine imbalance, due to either congenital inadequacy or deterioration due to advancing age, as the main cause of HFI. Calame (17) and Morel (18) also suggested dysendocrinism due to disturbance of the gonads (i.e., faulty estrogen stimulation, abnormal progesterone effect on the ovaries or inadequate androgen stimulation by the testis) as the most possible etiological factor in the development of HFI. These authors additionally speculated that the disturbance of the tubero-infundibular portion of the pituitary gland may influence the HFI formation, since the symptoms associated with HFI are the same as those of infundibulo-pituitary disturbance (e.g., adiposity, genital dystrophy, disturbance of sugar metabolism). They particularly emphasized gonadal factors and noted that male patients with HFI were commonly feminized, with atrophic testes. Having in mind the high prevalence and severity of HFI in females, HersHKovitz et al. (7) suggested that prolonged and/or increased estrogen stimulation during the reproductive period is the most probable cause of HFI. Hormonal disbalance in the etiology of HFI is not limited only to estrogens but on physiological balance of estrogens and androgens (12). HFI was related to altered androgen and pro-androgen levels (19), which result in estrogen/testosterone ratio changes. Thus, altered serum levels of estrogen in males were correlated with localized

ossification (20). Males developed extensive HFI due to extreme conditions of hormonal imbalance such as atrophied testes and resultant low levels of testosterone (7, 13). Namely, androgen suppression is potentiating the effects of estrogen on bone metabolism. Estrogen preserves bone mass, suppresses bone turnover, maintains balanced ratio bone formation/bone resorption, and functionally activates osteoclasts and osteoblasts (21). Results of the study in males who had chemical castration due to prostate cancer (22) showed that androgen suppression leads to surplus of estrogen, resulting in increased appearance of HFI. Additionally, researchers have reported lesions, similar to those encountered in HFI, after estrogen administration in mice (23).

Interestingly, it was observed, that HFI has much in common with breast cancer; increased and/or prolonged estrogen stimulus is associated with an elevated risk of breast cancer in humans as well as with the occurrence of HFI (7), both are primarily female phenomena, rise dramatically in frequency after menopause, associated with obesity and parity, and both the frontal bone and breast tissue are known to be target tissues for hormones such as estrogen and progesterone (24).

One of the latest speculations of HFI etiology, pointed increased leptin levels (peptide that signals the feeling of satiety to the hypothalamus and helps controlling the metabolic rate) as one of the possible factors that cause HFI (25). Serum leptin levels are correlated with body mass index and it was suggested that leptin has a certain influence on bone metabolism, such as positive relation between serum leptin levels and bone area especially influencing periosteal expansion in girls (26), but these effects are still debated. Ruhli (25) hypothesized that during human evolution, a wider ability of food favored an increased metabolic rate and increased leptin levels which may have lead to increase in an incidence of HFI.

1.5 HFI in historical and modern populations

The frequency of HFI differs greatly between studies conducted on the modern population and on population prior to the 19th century. Regardless of geographical location of population, HFI was rarity in populations prior the 19th century (7), while in modern era HFI was reported to appear with a considerable frequency (up to 46%) (27).

Therefore, the question imposes whether HFI is a long-standing phenomenon or is it a relatively new one characteristic for the modern era.

In an extensive research conducted on pre-19th century skulls, Hershkovitz et al. (7) did not find even a single case of HFI, whereas in an early 20th century collection they identified HFI in 12.8% cases. In a series of skeletal collections from 14th century BC to 17th century AD, a total frequency of HFI was just 2.49% (28). However, in one study performed on an osteological collection of Ancestral Pueblans (Anasazi) the overall frequency of HFI was 32.4% (29). This frequency rate is very similar to the results of the studies conducted on the last two centuries population. In order to explain this phenomenon, Ruhli et al. (30) hypothesized that the eating habits and lifestyle of these people had many similarities to those of the modern populations since they were inhabited in the ancient Pueblo Bonito which was a predominantly residence of wealthy people.

Some interesting suggestions have been offered in an effort to explain the higher frequency of HFI in modern population. The perception of increased frequency of HFI may be related to changes in life expectancy. Armelagos and Chrisman (31) stated that in this context shorter lifespan of the ancient populations should not be neglected.

Additionally, Hershkovitz et al. (7) stated that females born in the early 19th century were likely to manifest HFI in their postmenopausal life, unlike rare occurrence of HFI in historic populations, suggesting that the “turning point” was the industrial revolution which resulted in increased life span and changes in female lifestyle. Rapid urbanization reshaped the demographic characteristics of human populations, and consequently a new pattern of health and diseases emerged. May et al. (32) quoted that in females, hormonal disbalance occurs as a result of the changes in lifestyle such as a dramatic decrease in the number of children, shorter periods of breast feeding, extended reproductive period due to early onset of menarche and late onset of menopause. They stated that today’s females have almost tripled the number of cycles during their reproductive years (33) than females living 100 years ago. Hormonal alteration in modern females also may occur as a result of hormonal manipulation (i.e., contraceptives, hormonal replacement therapy) (34, 35). Finally, modern populations are exposed to hormones through different contaminated agents, such as consumption

of meat from animals treated with hormones (36) or consumption of dietary phytoestrogens from sources such as soy, grains and linseed (37).

1.6 Frontal bone

The frontal bone is one of the bones that forms the neurocranium, which serves as a protective case around the brain. The name “frontal bone” derives from the Latin word *frons* (meaning "forehead"). It is made of the vertical portion (squama frontalis) that forms the forehead and horizontal portion (pars orbitalis and pars nasalis) that forms the roofs of orbits and nasal cavity.

Frontal bone is a flat bone, composed of two thin layers of compact tissue (outer and inner tables) with a variable amount of cancellous tissue between them (diploe). The outer table is thick and tough, while the inner table is thin, dense and brittle. Red bone marrow is situated in the cavities of diploe (38).

Frontal region has specific vascularisation; soft and hard tissues form a separate angiosome. Dura matter of the anterior cranial fossa is vascularized from anterior meningeal branches of the anterior and posterior ethmoidal and internal carotid, and a branch from the middle meningeal artery (38). The veins returning the blood from the cranial dura mater anastomose with the diploic veins and end in the various sinuses (38).

The frontal bone is ossified intramembranously, from two primary centers, one for each half of the bone. These two primary centers are localized above each supraorbital margin. From each of these centers, ossification extends upward to form the corresponding half of the squama, and backward to form the orbital plate (38).

The mechanisms of the intramembranous ossification are still not completely understood (39). The skull is formed from cranial skeletogenic mesenchyme derived from two distinct embryonic sources: mesoderm and neural crest. The frontal bone is presumed to be derived from neural crest cells (40). The neural crest is a population of multipotent embryonic progenitor cells and plays an integral role in cranial morphogenesis as it

gives rise to osteoblasts. Specifically, the cranial neural crest is the sole source of the frontal bone primordium and its underlying dura mater (41).

Previous research didn't provide an adequate explanation why the frontal bone is particularly affected by HFI, however there are some suggestions that imply specific frontal bone involvement. Since it almost always begins in the middle third of the frontal squama, Morel (18) suggested that this localization might correspond to the primary centers of ossification of this bone. Hershkovitz et al. (7) supported this speculation due to the fact that these centers remain active bilaterally during adulthood. Estrogen stimulus may reactivate the primary centers of ossification of the frontal bone and cause abnormal bone growth (7). The bilateral occurrence of HFI, and the fact that the hyperostosis is limited to areas associated with the ossification centers and excludes both the midline area (metopic suture) and bregmatic area (anterior fontanel), lend further support to the notion of primary ossification center involvement (7).

1.7 HFI in relation to other skeletal sites

Previous studies have suggested that HFI is accompanied by increase of thickness of other cranial bones; Nikolic et al. (11) showed that increased bone thickness of frontal bone is followed by increase in temporal bones thickness as well. May et al. (42) demonstrated that women with HFI tend to develop more robust skull characteristics. Namely, in patient with HFI, cranial bones, brow ridge and external occipital protuberance became thicker with the increase of frontal bone involvement (42). The higher the grade of HFI was detected, the greater overall cranial bone thickening was present (42). Additionally, Kollin and Fehér (19) detected increased bone mineral content and bone width of the radius in women with HFI and pointed on a generalized alteration in morphology of the skeletal system in these women.

1.8 Symptoms of HFI

Although most of the patients with HFI are asymptomatic (43), the presence of HFI has a clinical relevance. Initially, HFI was considered one of the entities within

various clinical syndromes that affect multiple organ systems, such as: Morgagni-Stewart-Morel-Moore (obesity, virilism, neuropsychiatric symptoms, and headaches), Troell-Junet (acromegaly, toxic goiter, and diabetes mellitus), Frolich (obesity, growth retardation, pituitary hypocrinism) and Klippel-Trenaunay-Weber (varicose veins, port-wine stain, bone and soft tissue hypertrophy) (12). However, it can occur as an independent entity as well.

Researchers were investigating the possible relation of HFI and different symptoms that have been observed (mostly based on data from case reports) in patients with this condition. They have even speculated that hormonal-based conditions such as obesity and high insulin levels can lead to certain forms of skeletal ossifications and in this way correlated them with HFI (44). Blood sugar levels were reported to be slightly higher in patients with HFI (45) while HFI was reported twice as often in patients with diabetes (46). The possible connection between HFI and obesity was established by Morgagni (1). It was later reported that the prevalence of HFI is higher in obese patients (45, 47, 48). Adipose tissue converts testosterone to estradiol, thus HFI could be related to the adiposity due to increased production of estrogen by adipose tissue. Lahlou et al. (49) defined obesity as the primary resistance to circulating leptin, while Rhuli and Hanneberg (25) have even postulated a hypothesis that increased levels of leptin produce increase of bone overgrowth such as HFI.

Pawlikowski and Komorowski (50, 51) reported HFI in almost half of the women suffering from galactorrhoea, while Fulton (52) found HFI in more than half of the patients with acromegaly. Acromegaly is characterised by skeletal as well as soft tissue and skin overgrowth, due to increased growth hormone production. They showed strong association between pronounced HFI and these conditions and indirectly implied to the pituitary dysfunction origin of HFI. They explained that prolactin stimulates dehydroepiandrosterone production which leads to elevated levels of free testosterone and may result in menstrual troubles and hirsutism (52).

Latest research suggested that various symptoms may occur as a consequence of HFI (53). Namely, intrusive bone growth in patients with HFI may reduce intracranial volume or compress the cerebral cortex resulting in various symptoms (42). HFI is associated with cognitive slowing, mood disturbance, epilepsy, dementia,

schizoaffective disorders, headache and intracranial hypertension (7, 54). There are also studies that correlate HFI and Alzheimer's and Parkinson's disease (42, 55) as well as authors who correlated it with stroke (56).

The incidence of HFI was reported to be higher in emotionally disturbed women (53). Interestingly, Walinder (57) stated that incidence of mental morbidity was lower among siblings of mentally ill women with HFI than among siblings of mentally ill woman without HFI. This implies that HFI itself may be a cause of a certain disorders.

Devriendt et al. (54) speculated whether HFI causes brain atrophy through chronic cerebral compression or the bony nodules grow in order to occupy the intracranial space created by brain degeneration.

1.9 Pathogenesis of HFI

Over the years, several possible models of the HFI pathogenesis were presumed. The "American model" proposed by Moore (4), describes HFI as a process that triggers proliferation of spongy bone and that increase in diploic volume is pushing the inner table towards endocranial structures. The outer table is not affected due to its greater thickness and durability. The "European model" was proposed by Thevoz (58). He defined HFI as a process which transpires exclusively in the dura, and it is triggered by enlargement of the intradural vasculature. The most recent is the "global model" proposed by Hershkovitz et al. (7). According to this model HFI begins when osteogenic cells cause a disorganized diploization process in the inner table. These changes trigger the superimposition of newly formed lamellae on the inner table by the periosteum. The early compact hyperostosis is composed mainly of new lamellar bony layers deposited by the dura. Then, numerous blood vessels penetrate the lamellar bone from the dura, inducing bone proliferation. Over time, the original inner table becomes sclerotic and the newly formed bone undergoes dramatic reorganization with numerous large and irregular cavities (apparently blood sinuses). These enlarged cavities support the raised endocranial plate, which is recognized macroscopically as the remodeled overgrowth called HFI. Finally, the inner plate totally disappears; the reorganized bone

expands towards the diploic space and the cranial cavity, while only a thin shell of lamellar bone remains to envelopes the bulbous cavity.

According to global model, neither the external plate nor the diploe are directly involved since the bulging of the inner plate is primarily accruing due to newly formed lamellar bone produced by the endosteal dura. This opposes the statement of Perou (6) that “the diploe is primarily affected and pushes the inner table downward”. Both the European and the global model could be supported by a unique aspect of the frontal bone which is the adherence of the dura to its inner surface (7).

2 Research goals

The specific aims of the current thesis are:

1. To investigate differences in thickness of frontal, occipital and parietal bones between postmenopausal women with HFI and control group
2. To compare bone mineral density of hip and vertebral region, as well as external hip geometry between postmenopausal women with HFI and control group
3. To analyze differences in expression of cranial dural α -estrogen receptors between postmenopausal women with HFI and control group
4. To investigate micro-architectural difference of frontal bone among postmenopausal women with different types of HFI
5. To reevaluate current classification of HFI

3 Material and methods

This study comprised four research phases. The first phase included clinical study, second phase included immunohistochemical analyses of α -estrogen and CD34 receptors on dura, third phase included micro structural analyses of frontal bone samples and fourth phase included fractal analysis of the head computerized tomography (CT) scans in women with HFI.

3.1 Clinical study

The first phase was designed as a cross-sectional study. It was conducted in the Center for Radiological Diagnostics of School of Dental Medicine, University of Belgrade, in the period from 2011 to 2014. During this period, 739 women underwent computerized tomography (CT) of the head, done for diagnosis of chronic sinusitis. Only postmenopausal women (women who had their final menstrual period at least 12 months prior) with confirmed diagnosis of chronic sinusitis and who performed head CT scan for the first time were eligible to participate in this study. Exclusion criteria were presence of bone related pathologies other than HFI, as well as medical history of brain tumor, meningioma, renal diseases, primary hyperparathyroidism and Paget's disease. Thus, a total of 108 women were eligible according to these criteria (14.6%). The study sample comprised 103 women, because 3 women refused to complete a questionnaire, while 2 women refused to have a DXA scan performed (participation rate of the women approached was 13.9% and participation rate among those found eligible was 95.4%).

The presence of HFI was detected in 48 women (46.6%), among whom 28 had a moderate form and 20 had a severe form of HFI. Characteristics of the study population are given in the Table 1.

Table 1. Characteristics of the study population

<i>Parameter</i>	<i>Control group</i> <i>N=55</i> <i>(mean ± SD)</i>	<i>HFI</i> <i>N=48</i> <i>(mean ± SD)</i>
Mean age (years)	65.1±8.4	68.0±7.5
Mean age of menopause (years)	49.2±4.8	49.1±4.7
Mean height (cm)	160.4±6.7	160.2±6.1
Mean weight (kg)	69.8±13.9	74.4±12.5
Mean body mass index (kg/m²)	26.9±5.4	28.8±4.4

3.1.1 Head CT scans

All the CT images were processed using Somatom Sensation 16 (Siemens): slice thickness 3mm, parallel to the Frankfurt plane, 120kV, 300-400mAs, rotation time 0.4-0.5s, pitch 0.39, FOV 216mm, Matrix 512*512. To detect the presence of and to classify HFI, head CT scans were analyzed using volume rendering (VR) technique and multi-planar reconstruction from slices 0.75mm thick. Based on the head CT scan analyses results, all participants in the study were categorized as the control group (without HFI) and the group with HFI. Classification of patients with HFI in our study was based on the modification of Hershkovitz et al.'s (7) method. Women who demonstrated HFI were subdivided in two groups (Figure 1): moderate HFI (comprising types A and B by Hershkovitz et al.'s criteria) and severe HFI (comprising types C and D by Hershkovitz et al.'s criteria). To detect and classify the HFI, the intra-observer test was performed 3 times with 2-week intervals between each sample ranking. The inter-observer test was performed by three independent researchers. Kappa values were adequate at 0.725 and 0.783, respectively (59).

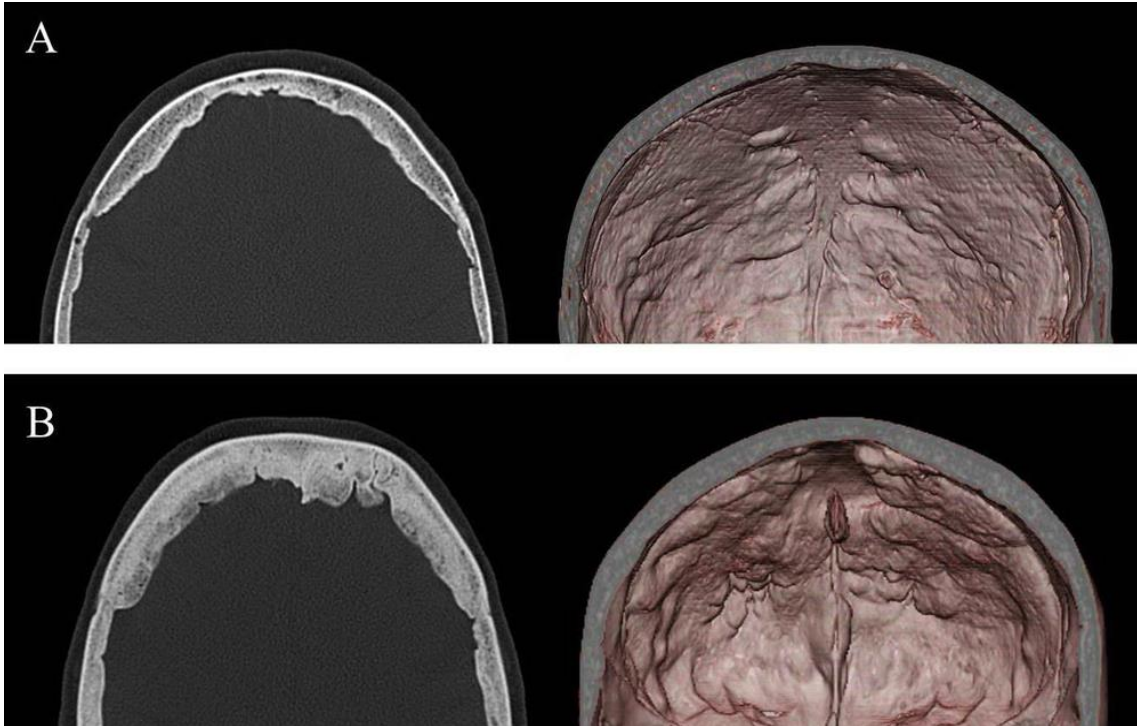


Figure 1. CT scans of the skull (**A**-moderate HFI, **B**-severe HFI). Axial scans in the bone window (left) and 3D reconstruction images (right), demonstrating the thickening of the inner table of the frontal bone.

3.1.2 Cranial bones thickness

The correlation between the presence of HFI and thickness of other cranial bones was assessed on head CT scans, by measuring frontal bone thickness (mm), parietal bones thickness (mm) and occipital thickness (mm). Using the sagittal plane in multiplanar reconstruction, we marked the level one centimeter above the most prominent point of glabella. Starting from this level, we used five successive transversal slices to measure the cranial bones thickness. Frontal and occipital bone thickness was measured 1 cm lateral to the mid-sagittal axes, perpendicular to the endocranial table surface (Figure 2). Left and right parietal bones thickness were measured 1cm anterior and posterior to the mid-transversal axes, perpendicular to the endocranial table surface (Figure 2). The mean thickness was used for each bone.

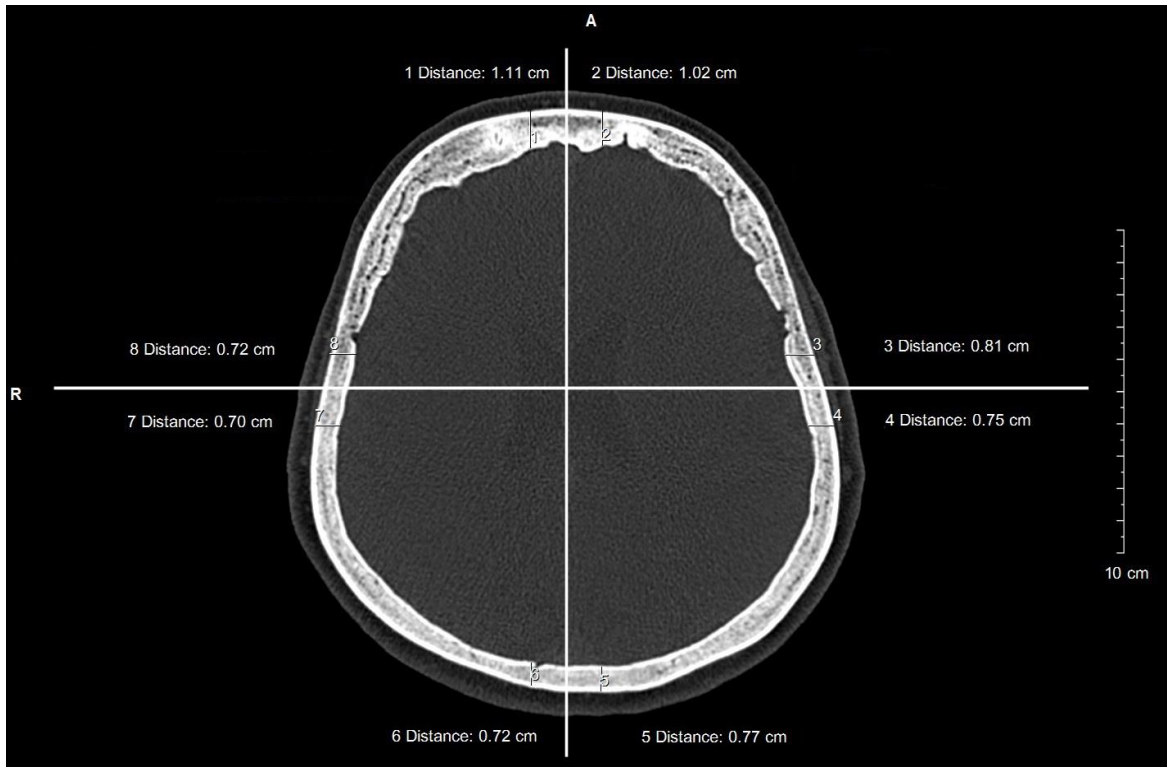


Figure 2. Measurement of the cranial bones thickness on the transversal CT scan of the head: frontal and occipital bone thickness (measured 1 cm lateral to the mid-sagittal axes, perpendicular to the endocranial table surface) and left and right parietal bones thickness (measured 1cm anterior and posterior to the mid-transversal axes, perpendicular to the endocranial table surface).

3.1.3 Symptoms and conditions related to HFI

Based on the data collected from the literature about the demographic characteristics, symptoms and conditions that could be related to HFI, we used an investigator-developed instrument to collect this information (Figure 3). Participants in this study were asked whether their menstrual cycles were regular, whether they had given birth, had breastfed, or had had galactorrhea, hirsutism, high blood pressure, neurological and psychiatric disorders, thyroid gland diseases, diabetes mellitus, headaches, memory loss, or unilateral hearing loss or had used hormonal contraceptives.

Naziv istraživanja: „Hiperostosis frontalis interna-moguća veza sa osteoporozom?“

UPITNIK ZA ISPITANIKE

1. Ime i prezime: _____
3. Starost: _____
4. Menstrualni ciklus: početak _____ kraj _____
5. Urednost: ne da
6. Porođaj: ne da _____
(kada i koliko)
7. Dojenje: ne da
8. Galaktoreja: ne da
9. Telesna visina: _____
10. Telesna težina: _____ BMI= _____
11. Dlakavost: ne da
12. Upotreba kontracepcije: ne da _____
(koliko dugo)
13. Upotreba druge hormonske terapije: ne da _____
(koje i koliko dugo)
14. Hipertenzija: ne da
15. Dijabetes: ne da
16. Štitna žlezda: ne da _____
17. Glavobolja: ne da
18. Poremećaj pamćenja: _____ (u poslednjih 10 god.)
19. Ostali psihički poremećaji (epilepsija, demencija): _____
20. Neurološki poremećaji: ne da _____
21. Naglupost: ne da _____ (najjednouvo)

Figure 3. Investigator-developed instrument used for data collection

3.1.4 DXA scans and HSA analyses

Within three months after the head CT scan, each patient included in the study had bone densitometry of the left hip and spine region performed by dual energy x-ray absorptiometry (DXA, Hologic Discovery C; S/N 83200). The scans were automatically evaluated by DXA software, providing values of bone mineral content (BMC; g), bone mineral density (BMD; g/cm²) and T (number of standard deviations that one's BMD

differs from the value normally expected in a healthy young adult of the same sex and ethnic origin) and Z scores (number of standard deviations that one's BMD differs from the value normally expected for someone of the same age, sex, weight, and ethnic origin), of the standard hip regions (neck and total) and spine lumbar region (total).

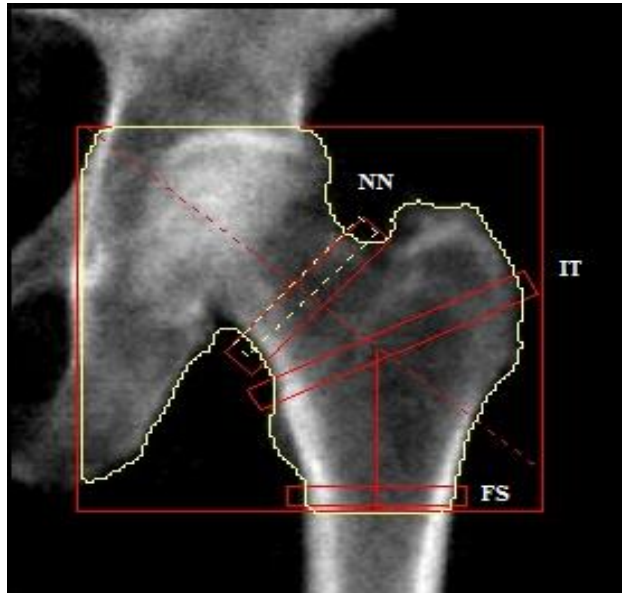


Figure 4. DXA scan image of the hip regions showing regions of interest used in hip structure analysis (NN- narrowest neck, IT- intertrochanteric region, FS- femoral shaft region)

To investigate the external geometry of the proximal femur, we used hip structure analysis (HSA) software developed by Beck and colleagues (60) and implemented it on Hologic software version 2.0 to calculate parameters of the femoral external geometry from the DXA scan. Three regions of interest corresponding to 5-mm-thick cross-sectional slabs of bone were assessed in this analysis: the narrowest neck (NN) located across the narrowest diameter of the neck, the intertrochanteric (IT) region traversing the bisector of the neck and shaft axes and the femoral shaft (FS) region located 1.5 times the neck width distal to the axes intersection (Figure 4). Outer diameter (OD, cm) and estimated cortical thickness (Ct. Th, cm) were calculated for each region of interest. Additionally, on each proximal femora hip axis length (HAL, mm) was measured (60).

3.2 Analyses of α -estrogen and CD34 receptors on dura

Dural tissue samples were collected during routine autopsies from human donor cadavers at the Institute of Forensic Medicine of the School of Medicine in Belgrade, in the period from 2014 to 2015. Exclusion criteria encompassed the presence of bone related pathological conditions other than HFI in the HFI group, as well as a history of brain tumor, meningioma, renal diseases, primary hyperparathyroidism and Paget's disease. The study sample comprised a group of 12 women with HFI (mean age: 68.4 ± 12.6) and an age-matched control group of 15 women (mean age 73.9 ± 10.8). Immunohistochemical analysis of α -estrogen and CD34 receptors was performed on 5 μ m sections which were prepared from the paraffin blocks. Sections (5- μ thick) from the formalin-fixed, paraffin-embedded tissue samples were deparaffinized and treated with 3% hydrogen peroxide for 15 min to block endogenous peroxidase activity. For the heat-induced antigen retrieval, tissue sections were immersed in 0.01 mol/l citrate buffer (pH=6.0) and treated in a microwave oven for 20 min at 620 W. After cooling off for 30 min at room temperature, blocking peptide (DAKO, Glostrup, Denmark) was utilized to block the non-specific staining. Thereafter, tissue sections were incubated overnight at 4°C with the following rabbit monoclonal primary antibodies: α -estrogen receptor (clone NCL-ER-6F11, dilution 1:100; ; Novocastra Laboratories Ltd, Leica Biosystems, Germany) and endothelial cell marker CD34 (clone NCL-L-END, dilution 1:100; Novocastra Laboratories Ltd, Leica Biosystems, Germany). Streptavidin-biotin technique using DAKO's LSAB+ kit (DAKO, Denmark) was applied, with diaminobenzidine (DAB) as the chromogen solution and Mayer's hematoxylin for the counterstain. Incubation with the pure antibody diluent (without the primary antibody) served as a negative control. As a external positive control for α -estrogen receptor immune staining we used breast carcinoma tissue. For CD34 external positive control was haemangioma. Nuclear staining for α -estrogen receptor and cytoplasmic expression for CD34 were treated as positive. The results of immunohistochemical staining for α -estrogen receptor were scored qualitatively by light microscopy as positive/negative. Microvessel density measurement was performed after CD 34 staining of the specimens. A modified Chalkley count method was utilized to measure microvessel density (61). Vascular hot- spots were selected and marked for each specimen. Using the Q Prodit

image analysing system (version 6.1; Leica, Cambridge, UK) with 30 micrometer grid lines the number of microvessels were counted within each separate hot-spots (magnification 40×) and results were presented as mean of the three counts.

3.3 Micro structural analysis

Frontal bone samples were collected during routine autopsies from human donor cadavers at the Institute of Forensic Medicine of the School of Medicine in Belgrade, in the period from 2014 to 2015. Exclusion criteria encompassed the presence of bone related pathological conditions other than HFI in the HFI group, as well as a history of brain tumor, meningioma, renal diseases, primary hyperparathyroidism and Paget’s disease.

Table 2. Characteristics of the study population

<i>Women with HFI</i>				<i>Control group</i>
Type A N=4	Type B N=4	Type C N=4	Type D N=8	N=14
74.1±9.7 (<i>mean ± SD</i>)				69.9±11.1 (<i>mean ± SD</i>)

The study sample comprised 34 women: 20 with HFI and 14 age-matched controls. We subdivided women with HFI in 4 groups, each group demonstrating different macroscopic type of HFI (Figure 5). Characteristics of the study population are provided in the Table 2.

Frontal bone samples of approximately 1 cm x 1 cm were harvested using slow rotating medical saw from the part where the frontal bone was the thickest (Figure 5). They were stored in 70% ethanol and cleaned of adherent soft tissue. Each frontal bone specimen was placed in a sample holder with a consistent orientation and scanned in dry

conditions by micro-computed tomography (Skyscan 1172, Bruker, Belgium). The micro-CT was operated at 80 kV, 124 μ A and 1200 μ s exposure time, with an isotropic resolution of 10 μ m and applied Al+Cu filter. The following regions of interest were determined for each investigated sample: total sample, outer table, diploe and inner table (Figure 6). The micro-architecture of the cortical and trabecular bone was evaluated automatically using micro-CT evaluation program CT.An with direct 3D morphometry. The threshold was set at 110/255. Investigated microstructural parameters for each region of interest were: total sample (bone volume fraction (BV/TV, %), outer table (bone volume fraction (BV/TV, %), pore diameter (Po.Dm, mm), total porosity (Po.Tot, %) and fractal dimension (FD)), diploe (bone volume fraction (BV/TV, %), trabecular number (Tb.N, 1/mm), trabecular thickness (Tb.Th, mm), trabecular separation (Tb.Sp, mm), structure model index (SMI), connectivity density (Conn.D, 1/mm³), degree of anisotropy (DA), total porosity (Po.Tot, %) and fractal dimension(FD)) and inner table (bone volume fraction (BV/TV, %), pore diameter (Po.Dm, mm), total porosity (Po.Tot, %) and fractal dimension (FD)).

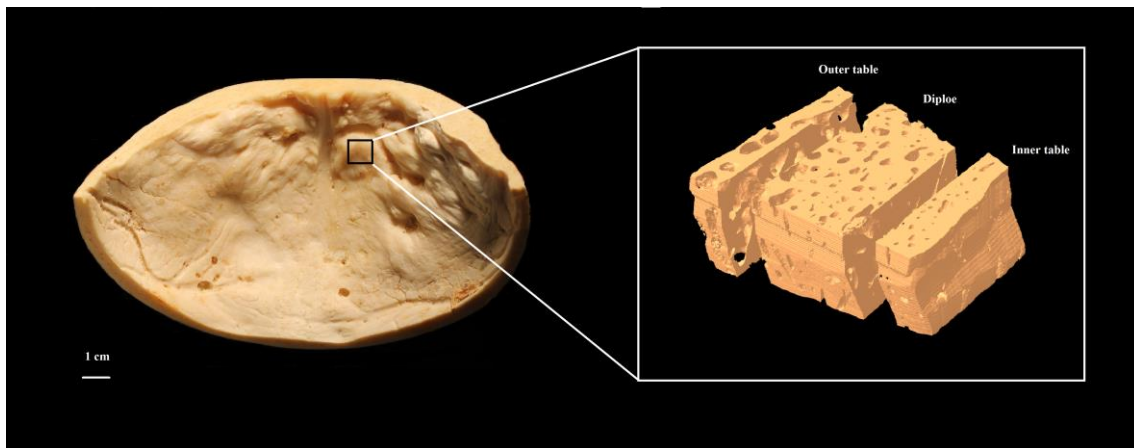


Figure 6. (left panel) A macroscopic view on the internal surface of the frontal bone in a woman with HFI (black rectangle shows the location of the analyzed frontal bone sample). (right panel) A 3D micro-computed tomography reconstruction in a woman with HFI, showing the segmentation of the frontal bone samples to the regions of outer table, diploe and inner table.

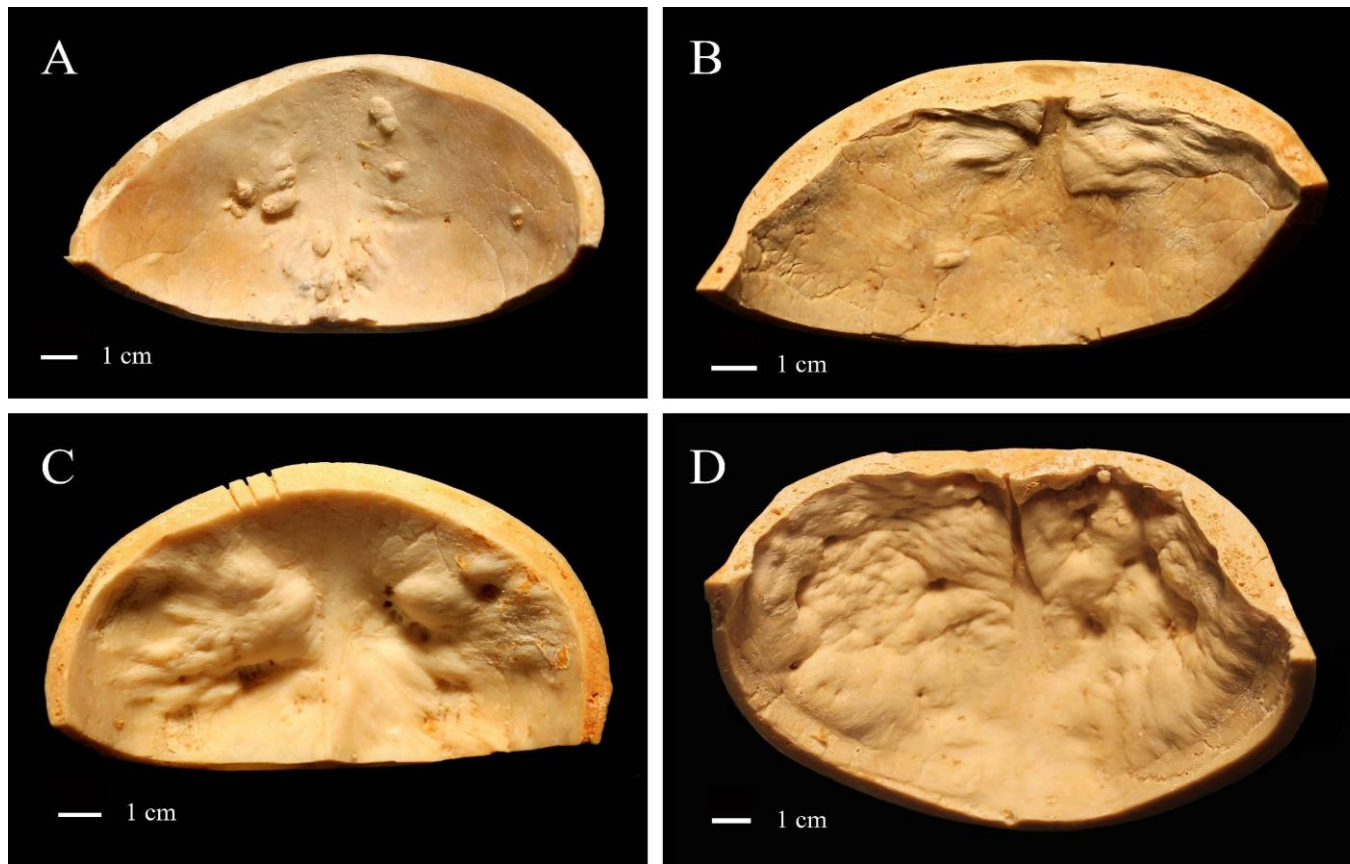


Figure 5. A macroscopic view on the internal surface of the frontal bone of women demonstrating different types of HFI (A-type A; B-type B; C-type C; D-type D)

3.4 Fractal analysis

Based on the head CT scan analyses results, women with HFI were divided in 4 groups, each demonstrating different type of HFI according to present macroscopical/radiological classification (type A, B, C and D) (7). In order to increase our study sample and the number of individuals within each group, we extended this research and continued data collection during 2015. Finally, the study sample included 73 women with HFI. Distribution of women within groups and mean age within each group are given in the Table 3.

Table 3. Characteristics of the study population

Type of HFI	HFI type A	HFI type B	HFI type C	HFI type D
Number of individuals within a group	N=9	N=19	N=22	N=23
Age (<i>mean</i> ± <i>SD</i>)	66.89±6.25	70.89±7.15	73.72±6.13	68.43±8.76

Using the sagittal plane in MPR, we marked the level one centimeter above the most prominent point of glabella, and used transversal slice in this level as a 2D representative of the head CT scan (Figure 7). When detecting and classifying the HFI, as well as determining the adequacy of classification based on representative transversal slice compared to 3D model in MPR, the results from three different radiologists were tested, and intra-observer testing was performed three times within a two-week interval between sample analyses by one of the radiologists. Kappa values were adequate at 0.725 and 0.783, respectively (59).

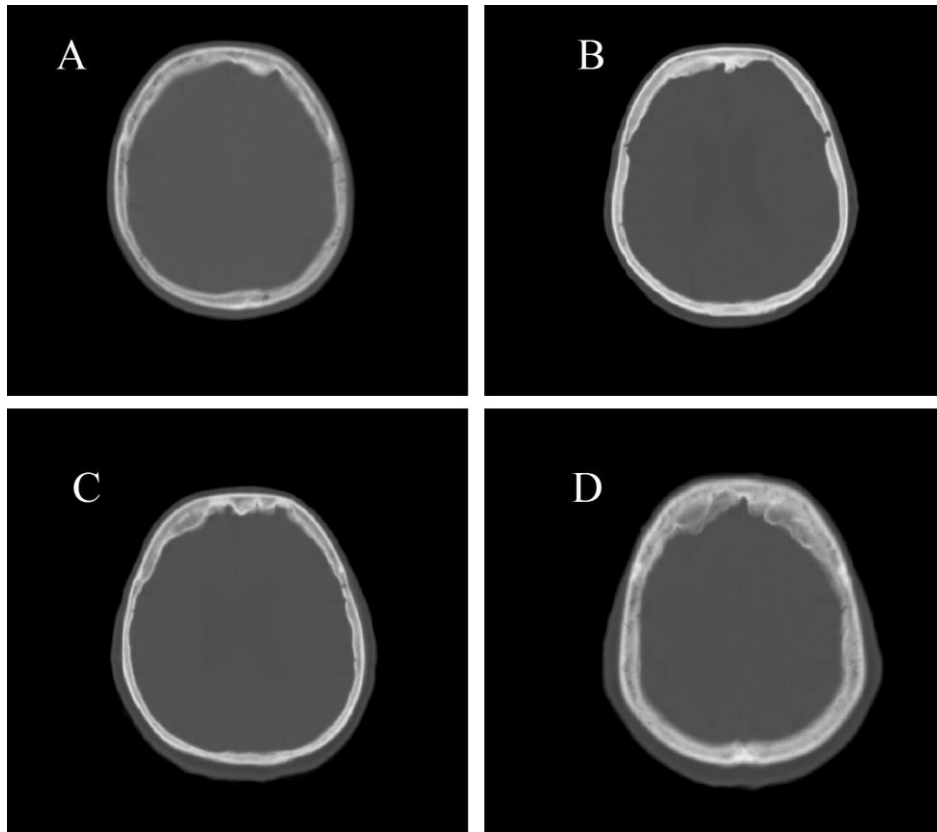


Figure 7. Representative transversal slice of the head CT of patients with different types of HFI (A, B, C and D)

In order to test current classification scheme of HFI we used previously defined transversal slices of the head CT scans of women with different types of HFI and performed fractal analyses of these images. HFI results in irregularity of the shape of the inner table of the frontal bone, and consequently the inner table of the skull. Using the fractal analysis we quantitatively analyzed the irregular shape of the inner table of the skull by counting two parameters: fractal dimension and circularity.

3.4.1 Digital image processing

An automated image analysis protocol was developed in software "Image J", specialized public domain software for image analysis, developed by the National Institutes of Health. Image processing procedure is illustrated in Figure 8. The first step is the conversion of RGB images into grayscale images (Figure 8A), followed by an adaptive threshold selection to get binary images (Figure 8B). Binary images were then additionally processed by image outline (Figure 8C) by calling outline from the

software "Image J" processing toolbox. Finally, the outer contour of the skull (corresponding to the outer table) was deleted while the inner contours of the skull (corresponding to the inner table) remained (Figure 8D).

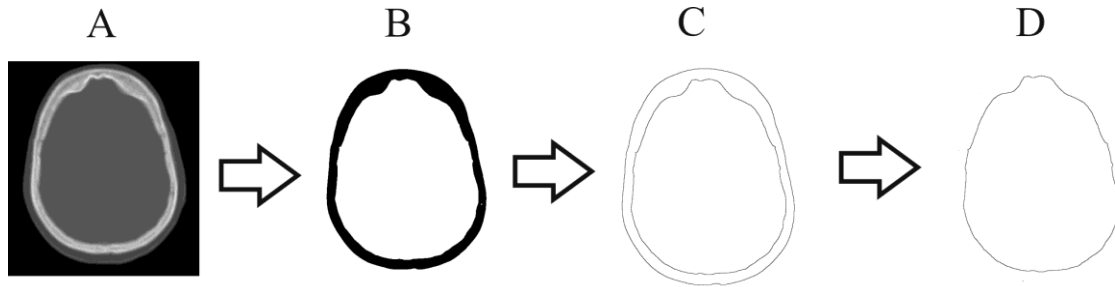


Figure 8. Scheme of the image processing procedure: the grayscale image (A), the binary image (B), the outline image (C) and the inner contour image (D).

3.4.2 Parameters of shape of the inner contour

The shape of the inner contour of the skull was numerically expressed, using two parameters of shape: the fractal dimension and the circularity. We tested present macroscopical classification of HFI by comparing these two parameters between groups with different types of HFI.

3.4.3 Fractal dimension of the inner contour

Fractal dimension of the inner contour (D) defines the irregularity of its shape, or precisely, how its shape deviates from the corresponding circle (fractal dimension of the circle is $D = 1.104$) (Figure 9A). The image of the inner contour was analyzed by the fractal analysis using the box-counting method (62, 63). This method consists of “covering” the image with sets of squares, with a precise length of the square edge (r) (Figure 9B). The number of squares (N) that covers or touches the inner contour of the skull is presented as a function of r (Figure 9C). D is determined from absolute slope value of the log–log relationship between $N(r)$ and r (Figure 9C). In performing the box-counting method, the box sizes are scaled to the base of 2; that is, $2^1, 2^2 \dots 2^k$, where

k continues until N is equal to unity. Depending on the contour image size, the box-sizes were taken from 2 to 512 or 1024 pixels.

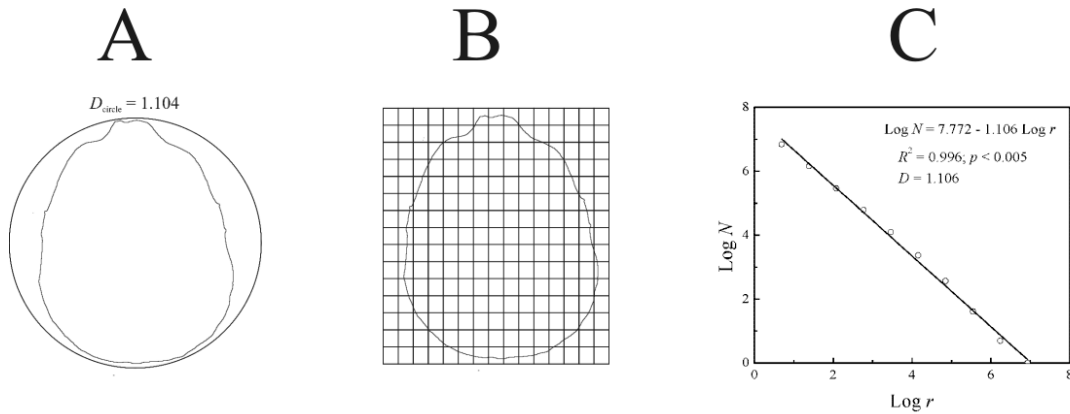


Figure 9. Illustration of the inner contour of the skull fractal dimension calculation. Fractal dimension of the circle is given in the upper part of figure (A). The application of the box-counting method to the inner contour: image is covered with a set of squares and the numbers of squares which cover the inner contour of the skull were counted (B). Log–log plot between numbers of squares (N) and square size (r) is fitted by a straight line (C). Obtained fractal dimension was 1.106 while R^2 is the corresponding determination coefficient and p is the significance level.

3.4.4 Circularity of the inner contour

The shape of the inner contour of the skull was estimated by using the parameter of circularity (C). This parameter represents a measure of given shape's deviation from a corresponding circle. The circularity equals one for a circle, while its value is less than one for any other shape. For the image of the inner contour this parameter was calculated according to formula $C = 4\pi AP^2$, where A is the area and P is the perimeter of the inner contour (Figure 10) (64).

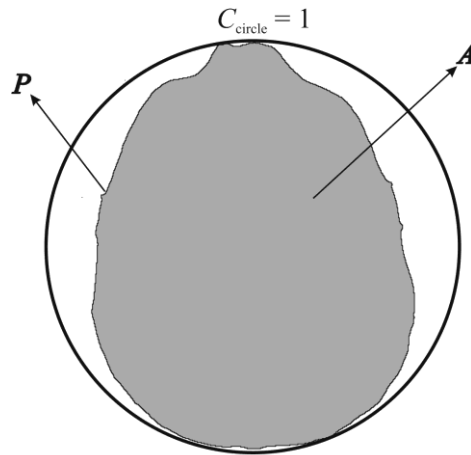


Figure 10. Illustration of the circularity of the inner contour of the skull calculation ($C = 4\pi AP^{-2}$, A is the area and P is the perimeter). Circularity of the circle is provided in upper part of figure.

3.5 Statistical analysis

For the clinical part of the study, the sample size was calculated using MedCalc statistical software ver. 9.1.0.1. (Sampling: Comparison of two means) with BMD neck being the primary outcome variable, type I error of 0.05, type II error of 0.20, observed standard deviation in both groups considered as measures of variability, and biologically relevant difference intended to be detected of at least 0.08 g/cm^2 (60, 65).

The Kolmogorov–Smirnov test was used to verify the normality of the data distribution.

One-way analysis of variance was used to evaluate the significance of the differences in the mean values of observed densitometric and external hip geometry parameters, as well as the thicknesses of the skull bones, between the women with HFI and the control group. The same analysis was used to compare these values between the control group and different stages of HFI. In post-hoc multiple comparison procedures, a Bonferroni adjustment was used, which set the significance level to $0.05/\text{number of comparisons}$. Given that the dimensions of the femur as well as the cross-sectional properties depend, at least partially, on bone size and age, all obtained data were

adjusted for standardized body height, weight and age to avoid the influence of these parameters on the results (60). Analysis of covariance was performed controlling for age, height and weight to assess differences in the means of all analyzed parameters between the groups. For multiple comparisons, a Bonferroni correction was used. To detect the association between thicknesses of cranial bones, a Pearson correlation was calculated. The association between the presence of HFI and prevalence of different symptoms and conditions was examined using the chi-square test.

When analyzing expression of CD34 receptor on cranial dura matter, differences in mean values (Chalkley count method) between the group of women with HFI and control group, independent samples T test was used.

Independent samples t-test was used to detect the differences in microstructural parameters between the group of women with HFI and control group. Paired samples t-test was used to evaluate the differences in microstructural parameters between the inner table and outer table in the group with HFI, as well as in control group. One-way analysis of variance (ANOVA) was used to assess the differences in microstructural parameters between the control group and different types of HFI, followed by post-hoc multiple-comparison procedures under Bonferroni correction.

Since the data within different groups were not normally distributed we used non-parametric test (Mann-Whitney test) to assess the differences in parameters of frontal bone shape (fractal dimension and circularity) between different types of HFI.

All analyses were conducted using SPSS statistical software (version 15.0) and the results were considered statistically significant at the 0.05 level.

4 Results

4.1 Clinical research

4.1.1 Symptoms and conditions related to HFI

Women with HFI showed significantly higher prevalence of headache, neurological and psychiatric disorders and a significantly lower prevalence of having given birth (Table 4). Mean number of childbirth in the group of women with HFI was 1.48 ± 1.22 , while in the control group it was significantly higher (1.70 ± 0.86). Among women with HFI, the most frequently reported neurological disorder was paresthesia (16.3%), and the dominant psychiatric disturbance was depression (16.3%). Additionally, patients reported conditions such as dizziness (6.2%), essential tremor (4.2%), dementia (4.2%) and different types of phobia (4.2%). The prevalence of prior breastfeeding, hirsutism, high blood pressure, diabetes mellitus, thyroid gland diseases, unilateral hearing loss, memory loss, hormonal contraceptives use and menstrual cycle regularity, did not differ significantly between the two groups of women. However, no woman in this study reported having ever had galactorrhea.

Additionally, our results showed that women with HFI had higher values of BMI and mean value of body weight (Table 1), but without statistical significance.

4.1.2 Cranial bones thickness

The thicknesses of the frontal, occipital and left and right parietal bones were significantly higher in the group of women with HFI compared to the control group (Table 5).

Table 4. Comparison of the distributions of conditions and symptoms between women with HFI and the control group

<i>Characteristic</i>		<i>Percentage</i>		<i>X² test</i>		
		<i>HFI</i>	<i>Control group</i>	<i>Value</i>	<i>Df</i>	<i>P</i>
Menstrual cycle regularity	Yes (%)	85.7	83.6	0.084	1	0.772
	No (%)	14.3	16.4			
Breastfeeding	Yes (%)	66.7	70.5	0.170	1	0.680
	No (%)	33.3	29.5			
Childbirth	Yes (%)	76.2	93.4	6.304	1	0.012*
	No (%)	23.8	6.6			
Galactorrhea	Yes (%)	0	0	/	1	/
	No (%)	100	100			
Hirsutism	Yes (%)	26.8	26.2	0.005	1	0.946
	No (%)	73.2	73.8			
Hormonal contraceptives use	Yes (%)	23.8	14.8	1.365	1	0.224
	No (%)	76.2	85.2			
High blood pressure	Yes (%)	73.8	67.2	0.514	1	0.473
	No (%)	26.2	23.8			
Diabetes mellitus	Yes (%)	21.4	19.7	0.047	1	0.828
	No (%)	78.6	80.3			
Thyroid gland diseases	Yes (%)	16.7	16.4	0.001	1	0.971
	No (%)	83.3	83.6			
Headache	Yes (%)	65.1	41.0	5.878	1	0.015*
	No (%)	34.9	59.0			
Memory loss	Yes (%)	57.1	41.0	2.604	1	0.107
	No (%)	42.9	59.0			
Psychiatric disorders	Yes (%)	23.8	6.6	6.304	1	0.012*
	No (%)	76.2	93.4			
Neurological disorders	Yes (%)	33.3	8.2	10.447	1	0.001*
	No (%)	66.7	91.8			
Unilateral hearing loss	Yes (%)	33.3	36.1	0.082	1	0.775
	No (%)	66.7	63.9			

Table 5. Means and standard deviations of the mean cranial bones thickness in the control group and in women with HFI

<i>Cranial bone</i>	<i>HFI</i>	<i>Control group</i>	<i>Sig.</i>
	<i>mean ± SD</i>	<i>mean ± SD</i>	<i>P</i>
<i>Frontal bone</i>	9.27±3.00	5.33±1.54	0.000*
<i>Occipital bone</i>	8.19±1.88	6.66±1.07	0.001*
<i>Parietal bone (left)</i>	7.18±2.04	5.32±0.84	0.000*
<i>Parietal bone (right)</i>	6.99±2.03	5.63±0.95	0.005*

Table 6. Means and standard deviations of the mean cranial bones thickness in the control group and in women with moderate and severe HFI

<i>Cranial bone</i>	<i>Control group</i>	<i>Moderate HFI</i>	<i>Severe HFI</i>
	<i>mean ± SD</i>	<i>mean ± SD</i>	<i>mean ± SD</i>
Frontal bone thickness (mm)	5.33±1.54 ^{a, b, c}	8.09±2.45	10.06±3.10
Occipital thickness (mm)	6.65±1.07 ^b	7.89±1.68	8.39±1.99
Left parietal bone thickness (mm)	5.32±0.84 ^{a, b}	6.37±1.68	7.71±2.09
Right parietal bone thickness (mm)	5.63±0.95 ^{a, b}	6.03±1.28	7.63±2.20

^a Significant difference (P<0.05) when compared moderate and severe HFI group

^b Significant difference (P<0.05) when compared control and severe HFI group

^c Significant difference (P<0.05) when compared control and moderate HFI group

We detected significant differences in thickness of all measured bones in the severe HFI group compared to the control group, but only the frontal bone was significantly thicker when the moderate HFI group was compared to controls (Table 6).

In the group of women with HFI, frontal bone thickness was positively correlated with the thickness of occipital, left and right parietal bones (Table 7).

Table 7. Correlation between frontal bone thickness and thickness of occipital, left and right parietal bones

		Occipital bone	Parietal bone (left)	Parietal bone (right)
Frontal bone	Pearson correlation	0.456*	0.544*	0.519*
	Sig. (2-tailed)	0.000	0.000	0.000

4.1.3 DXA scans and hip structure analyses

Unadjusted data revealed no significant statistical difference in bone density measurements between the group without and the group with HFI, except the vertebral Z score value, which was significantly higher in women with HFI (Table 8). However, after adjusting the densitometric parameters for age, height and weight, no statistically significant difference between the groups was detected (Table 9). Moreover, the results of the comparison of bone density parameters between the control group and patients with different forms of HFI also did not significantly differ in any site measured, after data adjustment (Table 10, 11).

External hip geometry parameters (outer diameter, cortical thickness and hip axis length) did not differ between the women with HFI and the control group or between women demonstrating different forms of HFI compared with controls (Table 8-11).

Table 8. Differences in densitometric and hip structure analysis parameters between control group and women with HFI (unadjusted data)

	<i>Unadjusted data</i>		
	<i>Control group</i>	<i>HFI</i>	<i>P</i>
	<i>N=55</i>	<i>N=48</i>	
	<i>mean ± SD</i>	<i>mean ± SD</i>	
BMC neck (g)	3.64±0.89	3.65±0.82	0.941
BMD neck (g/cm ²)	0.69±0.15	0.72±0.12	0.199
T score neck	-1.45±1.32	-1.12±1.08	0.178
Z score neck	0.11±1.31	0.52±1.03	0.081
BMC total (g)	28.47±6.12	29.31±5.48	0.471
BMD total (g/cm ²)	0.80±0.15	0.84±0.13	0.246
T score total	-1.13±1.23	-0.87±1.04	0.243
Z score total	0.15±1.19	0.52±0.99	0.089
BMC vertebral (g)	49.81±14.02	52.01±14.93	0.442
BMD vertebral (g/cm ²)	0.87±0.19	0.93±0.17	0.063
T score vertebral	-1.58±1.74	-1.01±1.54	0.083
Z score vertebral	0.10±1.80	0.92±1.60	0.015*
Outer diameter narrowest neck (cm)	3.36±0.28	3.42±0.33	0.319
Outer diameter intertrochanteric (cm)	5.53±0.36	5.67±0.43	0.060
Outer diameter femoral shaft (cm)	3.12±0.20	3.14±0.25	0.938
Cortical thickness narrowest neck (cm)	0.17±0.04	0.17±0.04	0.337
Cortical thickness intertrochanteric (cm)	0.34±0.08	0.35±0.06	0.208
Cortical thickness femoral shaft (cm)	0.49±0.12	0.51±0.10	0.369
Hip axis length (mm)	106.22±6.04	104.90±8.43	0.301

* p≤0.05 (significant differences between control and HFI group)

Table 9. Differences in densitometric and hip structure analysis parameters between control group and women with HFI (covariates appearing in the model are evaluated at the following values: age=66.45 years; height=160.30cm; weight=71.91kg)

	<i>Adjusted for age, height, and weight</i>		
	<i>Control group</i>	<i>HFI</i>	<i>P</i>
	<i>N=55</i>	<i>N=48</i>	
	<i>mean ± SE</i>	<i>mean ± SE</i>	
BMC neck (g)	3.70±0.10	3.59±0.11	0.463
BMD neck (g/cm ²)	0.70±0.01	0.71±0.02	0.483
T score neck	-1.37±0.13	-1.21±0.14	0.420
Z score neck	0.25±0.14	0.37±0.15	0.553
BMC total (g)	28.93±0.70	28.78±0.75	0.881
BMD total (g/cm ²)	0.81±0.01	0.83±0.02	0.527
T score total	-1.07±0.13	-0.94±0.13	0.516
Z score total	0.28±0.12	0.37±0.13	0.658
BMC vertebral (g)	50.75±1.81	50.94±1.94	0.944
BMD vertebral (g/cm ²)	0.88±0.02	0.92±0.02	0.288
T score vertebral	-1.43±0.19	-1.18±0.20	0.374
Z score vertebral	0.32±0.19	0.70±0.21	0.224
Outer diameter narrowest neck (cm)	3.38±0.04	3.41±0.04	0.619
Outer diameter intertrochanteric (cm)	5.55±0.05	5.65±0.05	0.152
Outer diameter femoral shaft (cm)	3.13±0.03	3.12±0.03	0.935
Cortical thickness narrowest neck (cm)	0.17±0.00	0.17±0.00	0.611
Cortical thickness intertrochanteric (cm)	0.34±0.01	0.35±0.01	0.405
Cortical thickness femoral shaft (cm)	0.49±0.01	0.50±0.01	0.650
Hip axis length (mm)	106.38±0.89	104.72±0.96	0.217

* p≤0.05 (significant differences between control and HFI group)

Table 10. Differences in densitometric and hip structure analysis parameters between control group and women with moderate and severe HFI

	<i>Unadjusted data</i>		
	<i>Control group</i>	<i>Moderate HFI</i>	<i>Severe HFI</i>
	<i>N=55</i>	<i>N=28</i>	<i>N=20</i>
	<i>mean ± SD</i>	<i>mean ± SD</i>	<i>mean ± SD</i>
BMC neck (g)	3.64±0.89	3.71±0.74	3.57±0.93
BMD neck (g/cm ²)	0.69±0.15	0.72±0.11	0.73±0.14
T score neck	-1.45±1.32	-1.14±0.96	-1.10±1.25
Z score neck	0.11±1.31	0.56±0.89	0.47±1.22
BMC total (g)	28.47±6.12	29.27±5.25	29.35±5.92
BMD total (g/cm ²)	0.80±0.15	0.82±0.12	0.86±0.14
T score total	-1.13±1.23	-0.98±0.98	-0.70±1.13
Z score total	0.15±1.19	0.45±0.93	0.62±1.09
BMC vertebral (g)	49.81±14.02	51.12±14.12	53.26±16.29
BMD vertebral (g/cm ²)	0.87±0.19	0.92±0.17	0.96±0.18
T score vertebral	-1.58±1.74	-1.17±1.51	-0.78±1.58
Z score vertebral	0.10±1.80*	0.82±1.53	1.05±1.53
Outer diameter narrowest neck (cm)	3.36±0.28	3.41±0.34	3.44±0.31
Outer diameter intertrochanteric (cm)	5.53±0.36	5.72±0.45	5.62±0.40
Outer diameter femoral shaft (cm)	3.12±0.20	3.16±0.28	3.10±0.23
Cortical thickness narrowest neck (cm)	0.17±0.04	0.17±0.03	0.18±0.04
Cortical thickness intertrochanteric (cm)	0.34±0.08	0.34±0.06	0.37±0.07
Cortical thickness femoral shaft (cm)	0.49±0.12	0.49±0.10	0.53±0.10
Hip axis length (mm)	106.22±6.04	104.71±5.66	105.15±11.42

*p≤0.05 (significant differences between control and moderate HFI group)

Table 11. Differences in densitometric and hip structure analysis parameters between control group and women with moderate and severe HFI (covariates appearing in the model are evaluated at the following values: age=66.45 years; height=160.30cm; weight=71.91kg)

	<i>Adjusted for age, height, and weight</i>		
	<i>Control group</i>	<i>Moderate HFI</i>	<i>Severe HFI</i>
	<i>N=55</i>	<i>N=28</i>	<i>N=20</i>
	<i>mean ± SE</i>	<i>mean ± SE</i>	<i>mean ± SE</i>
BMC neck (g)	3.70±0.10	3.64±0.14	3.52±0.17
BMD neck (g/cm ²)	0.70±0.01	0.71±0.02	0.71±0.02
T score neck	-1.37±0.13	-1.21±0.19	-1.22±0.22
Z score neck	0.25±0.14	0.41±0.19	0.31±0.22
BMC total (g)	28.93±0.70	28.66±0.98	28.94±1.15
BMD total (g/cm ²)	0.81±0.01	0.82±0.02	0.84±0.02
T score total	-1.07±0.13	-1.03±0.18	-0.83±0.21
Z score total	0.28±0.12	0.31±0.17	0.45±0.21
BMC vertebral (g)	50.752±1.81	49.88±2.54	52.41±2.99
BMD vertebral (g/cm ²)	0.88±0.02	0.90±0.03	0.94±0.03
T score vertebral	-1.43±0.19	-1.34±0.27	-0.95±0.31
Z score vertebral	0.32±0.19	0.56±0.27	0.82±0.32
Outer diameter narrowest neck (cm)	3.38±0.04	3.38±0.05	3.45±0.06
Outer diameter intertrochanteric (cm)	5.55±0.05	5.70±0.06	5.62±0.08
Outer diameter femoral shaft (cm)	3.13±0.03	3.14±0.04	3.10±0.05
Cortical thickness narrowest neck (cm)	0.17±0.00	0.17±0.01	0.17±0.01
Cortical thickness intertrochanteric (cm)	0.34±0.01	0.34±0.01	0.36±0.01
Cortical thickness femoral shaft (cm)	0.49±0.01	0.49±0.02	0.52±0.02
Hip axis length (mm)	106.38±0.89	104.12±1.25	105.55±1.47

4.2 Analyses of α -estrogen and CD34 receptors on dura

Only three of all analyzed samples of cranial dura expressed positivity for α -estrogen receptors (Figure 11), thus further analysis was impossible. However, immunohistochemical analysis of CD34 expression on cranial dura in women with HFI (Figure 13, 15) and control group was quantified using Chalkley count method and presented as mean of the three counts (Figure 12, 14). The results of this analysis showed significantly higher mean values of CD34 expression in the HFI group (Table 12).

Table 12. Differences in mean values of CD34 expression on cranial dura between women with HFI and control group

	<i>HFI (N=12)</i>	<i>Control group (N=15)</i>
<i>CD34 (mean \pm SD)</i>	8.42 \pm 2.54	5.67 \pm 11.59
<i>P</i>	0.02	

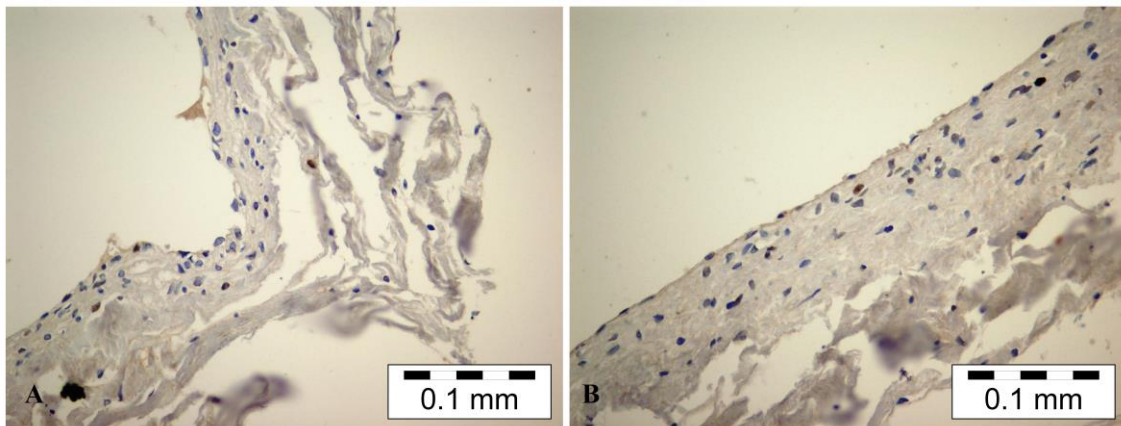


Figure 11. Immunohistochemical staining for α -estrogen receptors on dura samples (A-magnification 200 \times , B-magnification 400 \times)

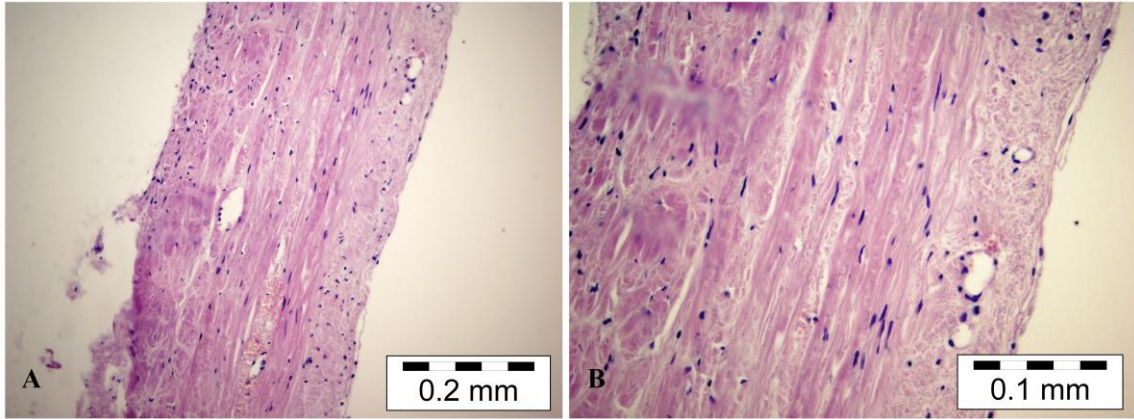


Figure 12. HE coloring of dura samples collected from the woman in the control group (A-magnification 200×, B-magnification 400×)

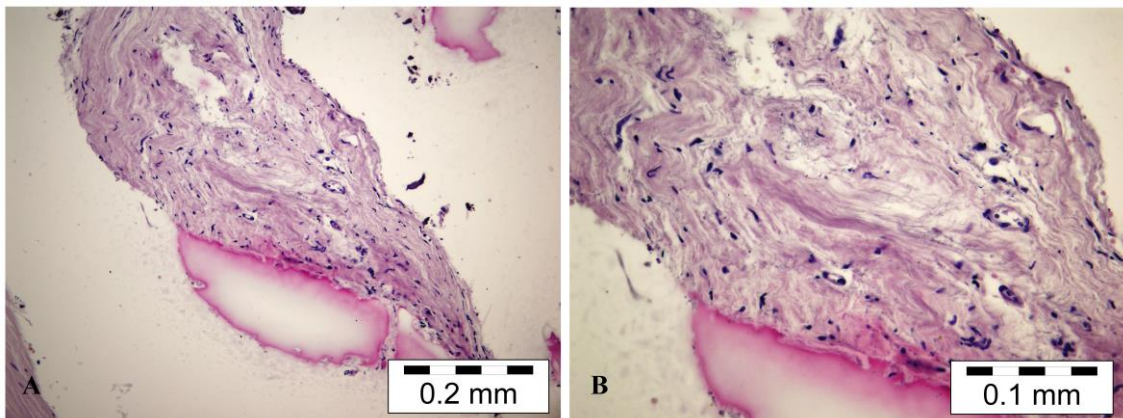


Figure 13. HE coloring of dura samples collected from the woman with HFI (A-magnification 200×, B-magnification 400×)

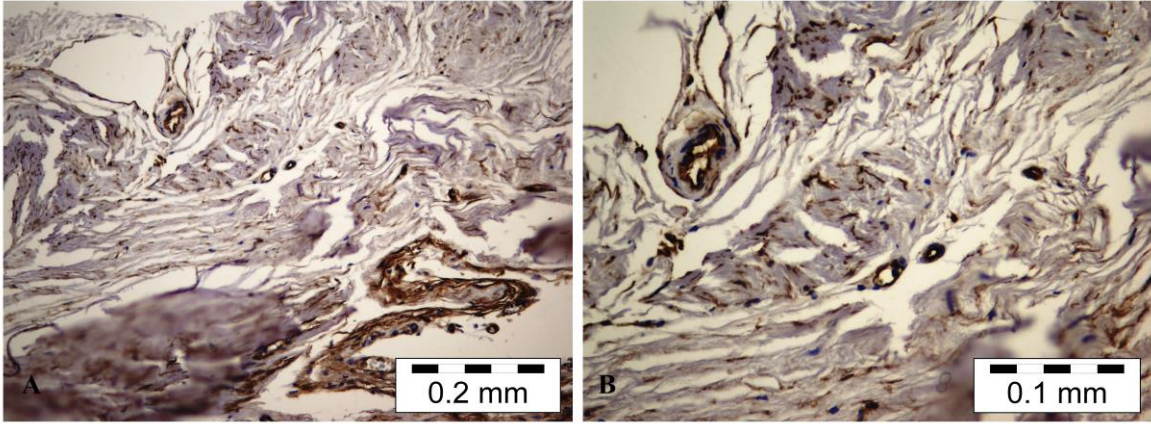


Figure 14. Immunohistochemical staining for CD34 receptors on dura samples collected from the woman in the control group (A-magnification 200×, B-magnification 400×)

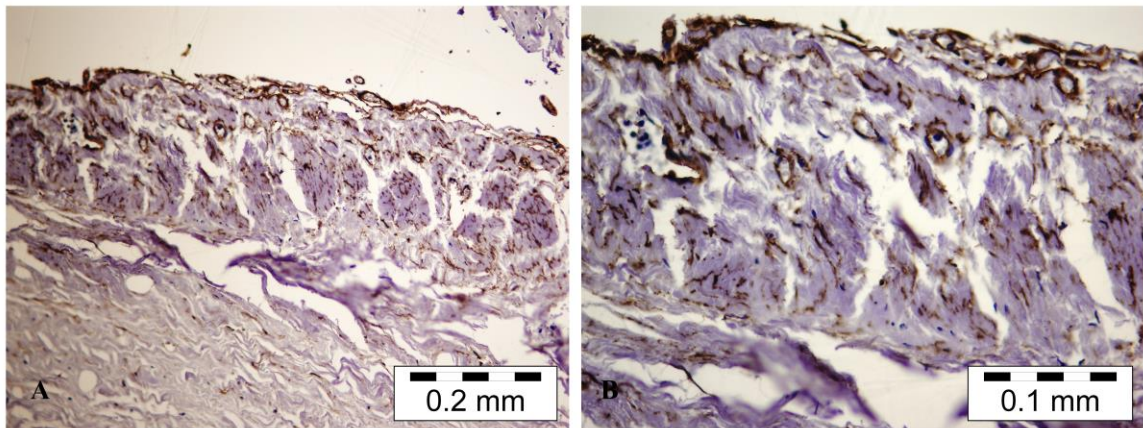


Figure 15. Immunohistochemical staining for CD34 receptors on dura samples collected from the woman with HFI (A-magnification 200×, B-magnification 400×)

4.3 Micro structural analysis

Bone volume fraction in women with HFI significantly increased in the region of diploe when compared to the control group (Table 13, Figure 16-18). No significant difference was detected in bone volume fraction either in the total sample or the regions of outer and inner tables. In the group of women with HFI the trabeculae were significantly thicker and more plate-like shaped in the region of diploe. Moreover, the trabecular separation and connectivity density significantly decreased in this region. In the region of inner table women with HFI demonstrated significant increase in total porosity (Table 13, Figure 16-18).

When analyzing the differences between the control group and types A, B, C and D of HFI significant differences were detected only in the region of diploe (Table 14, Figure 19). Overall, bone volume fraction in diploic region differed significantly between the investigated groups, but the multiple-comparison procedures revealed no significant differences in mean values between the individual groups. Structural model index and trabecular thickness in the region of diploe differed significantly between the groups, with post-hoc tests revealing significant inter-group difference between the control group and the type D of HFI (Table 14).

Since the comparison between the control group and different types of HFI reported only significant differences between the control group and type D of HFI, we reclassified the group with HFI into two groups: moderate HFI (comprising original types A, B and C) and severe HFI (type D). When comparing the control group with the groups of moderate and severe HFI, significant inter-group differences were detected in the region of diploe and inner table (Table 15). Namely, in the region of diploe bone volume fraction and trabecular thickness were significantly higher in the group of severe HFI than in the control group, while structural model index and connectivity density showed significantly lower values in the group of severe HFI compared to the controls (Table 15). Total porosity in the region of inner table was generally affected by the group, while post-hoc multiple comparisons revealed again significant inter-group differences only between the control and severe HFI groups.

Table 13. Differences of microstructural parameters between control group and women with HFI in different regions of frontal bone

<i>Microstructural parameters</i>	<i>Control group (N=14)</i>	<i>HFI (N=20)</i>
Total sample		
BV/TV	62.33±11.63	69.53±10.68
Outer table		
BV/TV	95.06±1.55	95.06±2.38
Po.Dm	0.08±0.01	0.08±0.03
FD	2.38±0.05	2.40±0.06
Po.Tot	4.94±1.55	4.94±2.38
Diploe		
BV/TV ^a	46.07±11.19	56.12±13.03
SMI ^a	-1.02±1.75	-2.74±2.57
Tb.Th ^a	0.23±0.03	0.27±0.06
Tb.N	1.96±0.33	2.09±0.40
Tb.Sp ^a	0.52±0.14	0.44±0.11
DA	1.95±.54	2.09±0.69
FD	2.60±.06	2.60±0.05
Po.Tot	50.36±16.99	43.87±13.03
Conn.D ^a	39.96±17.74	27.28±14.51
Inner table		
BV/TV	93.32±4.09	89.67±6.47
Po.Dm ^a	0.08±0.03	0.11±0.03
FD	2.31±0.09	2.37±0.10
Po.Tot ^a	5.46±3.09	10.27±6.49

Abbreviations: BV/TV (bone volume fraction, %), Po.Dm (pore diameter, mm), FD (fractal dimension), Po.Tot (total porosity, %), Tb.N (trabecular number, 1/mm), Tb.Th (trabecular thickness, mm), Tb.Sp (trabecular separation, mm), SMI (structure model index), Conn.D (connectivity density, 1/mm³), DA (degree of anisotropy)

^a Significant difference between the groups; t test, $p < 0.05$

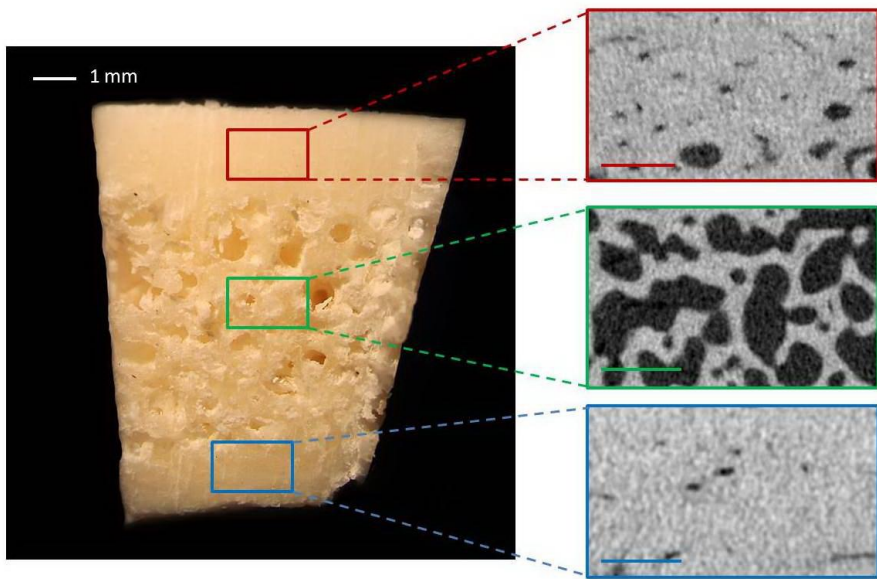


Figure 16. A macroscopic view of the frontal bone sample of woman from control group (left). Cross-section micro-computed tomography images of the frontal bone outer table (red square), diploic region (green square) and inner table (blue square).

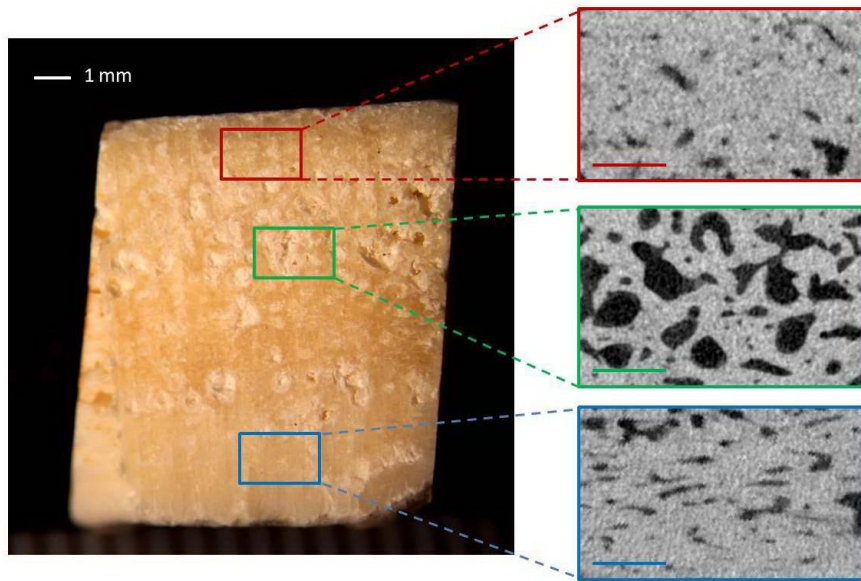


Figure 17. A macroscopic view of the frontal bone sample of woman with HFI (left). Cross-section micro-computed tomography images of the frontal bone outer table (red square), diploic region (green square) and inner table (blue square).

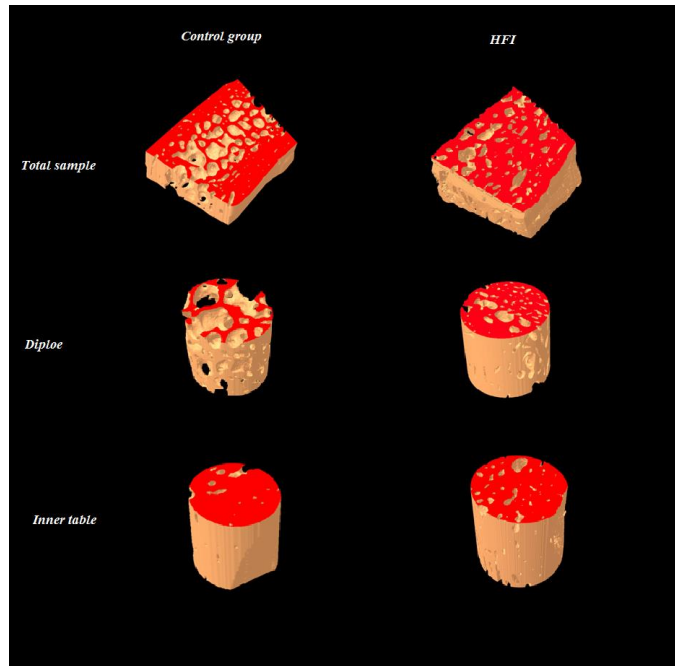


Figure 18. Representative 3D micro-computed tomography reconstructions of the frontal bone in women with HFI and control group. Note between-group differences in the regions of diploe and inner table.

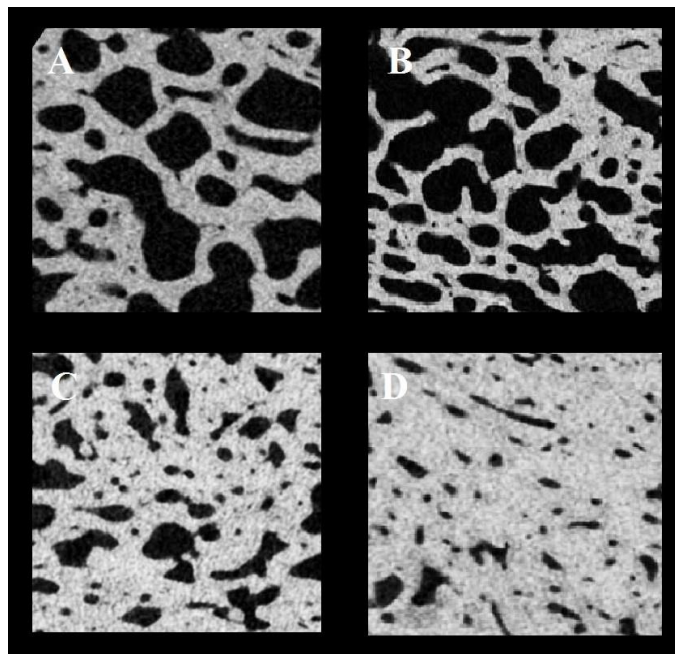


Figure 19. Cross-section micro-computed tomography images of the diploic region of the frontal bone in women demonstrating different macroscopic types (A, B, C and D) of HFI

Table 14. Differences of microstructural parameters between control group and types A, B, C and D of HFI in different regions of frontal bone

<i>Microstructural parameters</i>	<i>Control group (N=14)</i>	<i>HFI type A (N=4)</i>	<i>HFI type B (N=4)</i>	<i>HFI type C (N=4)</i>	<i>HFI type D (N=8)</i>
Total sample					
BV/TV	62.33±11.63	78.11±6.11	65.18±6.52	68.58±7.29	67.90±14.01
Outer table					
BV/TV	95.06±1.55	95.72±1.14	93.79±1.93	96.38±1.00	94.71±3.24
Po.Dm	0.08±0.01	0.08±0.02	0.10±0.01	0.08±0.01	0.08±0.04
FD	2.38±0.05	2.42±0.04	2.43±0.04	2.40±0.05	2.39±0.08
Po.Tot	4.94±1.55	4.28±1.14	6.21±1.93	3.61±1.00	5.29±3.24
Diploe					
BV/TV ^b	46.07±11.197	62.79±11.84	48.71±11.55	47.86±8.83	60.63±13.84
SMI ^a	-1.02±1.75	-2.83±1.74	-1.23±1.28	-1.58±1.00	-4.04±3.40
Tb.Th ^a	0.23±0.03	0.27±0.06	0.24±0.07	0.25±0.03	0.30±0.06
Tb.N	1.96±0.33	2.43±0.76	2.03±0.11	1.93±0.31	2.02±0.24
Tb.Sp	0.52±0.14	0.35±0.15	0.44±0.29	0.53±0.85	0.43±0.88
DA	1.95±0.54	2.16±0.58	2.57±1.01	1.90±0.49	1.90±0.66
FD	2.60±0.06	2.62±0.07	2.56±0.05	2.59±0.04	2.61±0.04
Po.Tot	50.36±16.99	37.20±11.84	51.28±11.55	52.14±8.83	39.37±13.84
Conn.D	39.96±17.74	36.74±21.05	32.75±21.20	28.07±8.94	19.42±3.92
Inner table					
BV/TV	93.32±4.09	92.62±3.96	88.21±7.41	91.42±2.83	88.04±8.30
Po.Dm	0.08±0.03	0.1±0.03	0.12±0.01	0.12±0.03	0.11±0.05
FD	2.32±0.09	2.40±0.07	2.28±0.04	2.36±0.09	2.41±0.12
Po.Tot	5.46±3.09	7.37±3.96	11.78±7.41	8.57±2.83	11.82±8.38

Abbreviations: BV/TV (bone volume fraction, %), Po.Dm (pore diameter, mm), FD (fractal dimension), Po.Tot (total porosity, %), Tb.N (trabecular number, 1/mm), Tb.Th (trabecular thickness, mm), Tb.Sp (trabecular separation, mm), SMI (structure model index), Conn.D (connectivity density, 1/mm³), DA (degree of anisotropy)

^a Significant difference between the control group and type D of HFI; ANOVA, $p < 0.05$

^b Significant overall inter-group differences but not between individual groups; ANOVA, $p < 0.05$

Additionally, comparing microstructural parameters between the outer and inner tables in the group with HFI revealed a significantly higher porosity and lower bone volume fraction in the inner table compared to the outer table. No significant differences in these parameters were detected between the regions of inner and outer tables in the control group. Distribution of pore diameter in women with HFI suggests that increased porosity in the inner table compared to outer table occurs due to higher

number of large pores (>100 μ m). Figure 20 shows the distribution of pore diameter in the inner and outer table in women with HFI.

Table 15. Differences of microstructural parameters between control group, moderate form of HFI (comprising types A, B and C of HFI) and severe HFI (type D of HFI)

<i>Microstructural parameters</i>	<i>Control group (N=14)</i>	<i>Moderate HFI (types A, B and C) (N=12)</i>	<i>Severe HFI (type D) (N=8)</i>
Total sample			
BV/TV	62.33 \pm 11.63	70.62 \pm 8.30	67.90 \pm 14.01
Outer table			
BV/TV	95.06 \pm 1.55	95.30 \pm 1.72	60.63 \pm 13.84
Po.Dm	0.08 \pm 0.01	0.08 \pm 0.02	0.08 \pm 0.04
FD	2.38 \pm 0.05	2.42 \pm 0.04	2.39 \pm 0.08
Po.Tot	4.94 \pm 1.55	4.70 \pm 1.72	5.29 \pm 3.24
Diploe			
BV/TV ^a	46.07 \pm 11.19	53.12 \pm 12.12	60.63 \pm 13.84
SMI ^a	-1.02 \pm 1.75	-1.88 \pm 1.44	-4.04 \pm 3.40
Tb.Th ^a	0.23 \pm 0.03	0.25 \pm 0.05	0.30 \pm 0.06
Tb.N	1.96 \pm 0.33	2.13 \pm 0.48	2.02 \pm 0.24
Tb.Sp ^a	0.52 \pm 0.14	0.44 \pm 0.12	0.43 \pm 0.88
DA	1.95 \pm .54	2.21 \pm 0.72	1.90 \pm 0.66
FD	2.60 \pm 0.06	2.59 \pm 0.06	2.61 \pm 0.04
Po.Tot	50.36 \pm 16.99	46.88 \pm 12.12	39.37 \pm 13.84
Conn.D ^a	39.96 \pm 17.74	32.52 \pm 16.70	19.42 \pm 3.92
Inner table			
BV/TV	93.32 \pm 4.09	90.75 \pm 5.02	88.04 \pm 8.30
Po.Dm ^a	0.08 \pm 0.03	0.11 \pm 0.03	0.11 \pm 0.05
FD	2.31 \pm 0.09	2.35 \pm 0.08	2.41 \pm 0.12
Po.Tot ^a	5.46 \pm 3.09	9.24 \pm 5.02	11.82 \pm 8.38

Abbreviations: BV/TV (bone volume fraction, %), Po.Dm (pore diameter, mm), FD (fractal dimension), Po.Tot (total porosity, %), Tb.N (trabecular number, 1/mm), Tb.Th (trabecular thickness, mm), Tb.Sp (trabecular separation, mm), SMI (structure model index), Conn.D (connectivity density, 1/mm³), DA (degree of anisotropy)

^a Significant difference between control group and severe HFI; ANOVA, p < 0.05

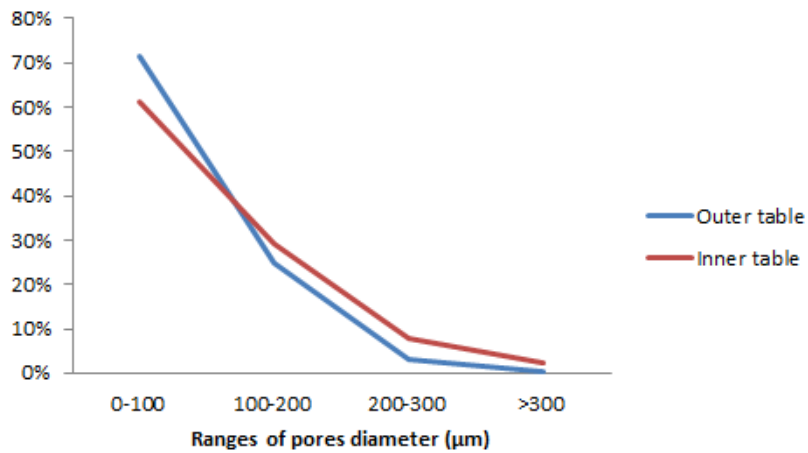


Figure 20. The distribution of pore diameters in the inner and outer tables in women with HFI. Note the dominance of larger pores in the inner table.

4.4 Fractal analysis

Mean values of parameters of shape (fractal dimension (D) and circularity (C)) are provided in the Table 16. Data show that all four types of HFI have similar values of the fractal dimension while type D of HFI has the smallest value of circularity in comparison to the other three types of HFI (A, B, and C).

Table 16. Mean values and standard deviations of the fractal dimension (D) and circularity (C) for types A, B, C, and D of HFI.

<i>Type of HFI</i>	<i>Fractal dimension (mean ± SD)</i>	<i>Circularity (mean ± SD)</i>
A	1.16 ± 0.04	0.83 ± 0.03
B	1.15 ± 0.03	0.83 ± 0.04
C	1.16 ± 0.03	0.82 ± 0.04
D	1.16 ± 0.03	0.74 ± 0.09

Values of parameters of shape were tested between four different types of HFI (Table 17). Reported results showed that between four types of HFI there is no

significant difference in the fractal dimension. However, values of circularity significantly differed when compared type D of HFI to types A, B and C of HFI. Analysis of circularity of the inner contour suggested that types A, B and C of HFI do not significantly differ from each other. These three types (A, B and C) could be considered as a unique type (moderate form of HFI), while type D of HFI should remain a separate type (severe form of HFI). Additionally, significant difference in values of circularity remained when we compared severe form of HFI (type D) to the moderate form of HFI (comprising types A, B and C).

Table 17. Distribution of the parameters of shape over pairs of samples tested for significance

<i>Compared types of HFI</i>	<i>Fractal dimension</i>		<i>Circularity</i>	
	<i>Z</i>	<i>p</i>	<i>Z</i>	<i>p</i>
Type A to type B of HFI	-1.182	0.237	-0.271	0.786
Type A to type C of HFI	-0.784	0.433	-0.152	0.879
Type A to type D of HFI	-0.084	0.933	-2.453	0.014*
Type B to type C of HFI	-0.785	0.432	-0.641	0.522
Type B to type D of HFI	-1.188	0.235	-3.236	0.001*
Type C to type D of HFI	-0.386	0.699	-3.419	0.001*
Moderate form (types A, B and C) to severe form of HFI (type D)	-0.784	0.433	-4.003	0.000*

5 Discussion

Eventhough HFI was considered one of the entities within different clinical syndromes (Morgagni-Stewart-Morel-Moore, Troell-Junet, Frolich, Klippel-Trenaunay-Weber), latest research suggested that various symptoms may occur as a consequence of HFI independent of these syndromes (53). Systematic recording of HFI in medical records can be helpful in distinguishing whether reported disorders occur as a consequence of HFI or are related to other diseases.

In our study, women with HFI reported a significantly higher prevalence of headaches, neurological and psychiatric disorders than controls. Previous studies based on case reports have also reported similar findings. Kocbah et al. (66) suggested that HFI is accompanied with epilepsy and dementia, Chaljub et al. (67) reported women with HFI who demonstrated schizoaffective disorder and memory loss, while Devriendt et al. (54) pointed out that almost all the patients with HFI had behavioural disturbances and were under psychiatric care. Ramchandren and Liebeskind (14) considered that the significantly higher prevalence of headache can appear as a result of altered hormonal influence in the patients with HFI, while other investigators have related it to the frontal bone compression on the cerebral cortex (68). Prominent forms of HFI may compress soft tissues with resultant dural irritation and pressure atrophy of the brain (69). In the research performed by Attansaio et al. (53) patient with HFI exhibited cortical atrophy extending to the frontal, temporal, and parietal lobes, and they attributed severity of their patient's psychiatric disorders to the extension of HFI and the level of cortical atrophy. In the cases of severe headaches in patients with HFI, the relief of the symptoms sometimes could only be accomplished by surgical decompression (69). In our study, the rate of women who reported headache as a symptom should be interpreted with caution, because the study sample included women who had a diagnosis of sinusitis, which might be accompanied by headache as well (70). The prevalence of HFI has been reported to be higher in emotionally disturbed women and women with psychiatric disorders (69), which was confirmed by our results as well, with depression as the most frequently reported disorder. We also observed that women with HFI had a significantly lower prevalence of having given birth. Pregnancy and nursing are

decreasing estrogen exposure (32), which implies that women with HFI were under increased estrogen stimulation. In historic populations women demonstrated different reproductive patterns (later menarche, earlier menopause and spent most of their reproductive life either pregnant or nursing) which have resulted in decreased estrogen exposures. Hence, the increase in frequency of HFI could be related to increased estrogen stimulation due to women altered reproductive behavior (7, 53).

Unlike previous studies (50), which reported HFI in 43% of women with galactorrhea and almost the same frequency in the group of women with hyperprolactinaemia (51), we haven't reported a single case of galactorrhoea in our study. Additionally, our results do not support the suggested speculation of the role of adipose tissue and leptin in the HFI development. The value of BMI was slightly higher in the HFI group of women but without significant differences. Therefore testosterone to estrogen conversion by adipose tissue and leptin induced bone formation are unlikely to be responsible for the HFI.

Apart from thicker frontal bone compared to women without HFI, women with HFI in our study had thicker occipital and parietal bones as well. Additionally, our results suggest that frontal bone was the first one to thicken, followed by parietal and occipital bones respectively. With the increase of the frontal bone thickness, the entire skull appeared to be thicker. Our findings are in accordance with the results of previous studies (22, 42, 71). These authors stated that a general increase in the cranial bone thickness causes reduced intracranial volume and suggested that presence of HFI might be correlated with the decreased brain volume. They hypothesized that the higher is the grade of HFI, the greater is the overall cranial bone thickening and the resultantly smaller intracranial volume (ICV), suggesting that HFI is somehow associated with a brain volume reduction process. Data in the literature showed correlation between intelligence and human brain size in elderly patients (72), hence in this context the presence of HFI may imply deterioration in mental abilities. Additionally, any cranial change that reduces brain size (such as HFI) may imply brain vulnerability (42). Additionally, our results indicated that the frontal bone might be the first one to thicken, followed by parietal and occipital bones respectively. These findings support the

suggestion made by Moore (4) who considered HFI and HCD to be different manifestations of the same process, with HFI occurring first, as a precursor to HCD.

Having in mind that the highest incidence of HFI is observed in women in the menopause, and in males with conditions resulting in decreased androgen stimulation, the role of sex steroids in development of HFI has been widely speculated (7, 19, 32, 42, 60). Additionally, the bone changes, similar to those defined as HFI, have been detected after estrogen administration in experimental animals (23). The presumptions of the influence of altered sex steroids on the formation of HFI, mostly rely on the effects of these hormones on bone metabolism. Sex steroid dysendocrinism through life, not only limited to estrogens, but on physiological balance of estrogens, progesterone and androgens, is pointed out as the most probable cause of HFI.

In both sexes, estrogen plays a central role in the regulation of bone metabolism by conserving bone mass, suppressing bone turnover and maintaining balanced rates of bone formation and resorption. It affects functional activity of both osteoclasts and osteoblasts (it decreases osteoclast formation and activity by increasing its apoptosis) (73, 74). Osteoblasts, osteoclasts and osteocytes contain functional estrogen receptors (estrogen α receptor- $Er\alpha$; estrogen β receptor- $Er\beta$), although their concentration is lower than in reproductive tissues. $Er\alpha$ mediates most of the actions of estrogen on bone cells, whereas $Er\beta$ can even act as a negative antagonist to $Er\alpha$ (75, 76). Bone cells contain both receptors, although their distribution within bone differs. $ER\alpha$ is predominantly localized in the cortical bone while $Er\beta$ in the cancellous bone (77). The major effect of testosterone on bone metabolism is reduction of bone resorptions, in addition to increasing the lifespan of osteoblasts and osteoclasts. Consequently, testosterone increases bone formation (74, 78). Testosterone accomplishes most of its action indirectly, via aromatization of testosterone to estrogen. Like estrogen, testosterone also increases the lifespan of both osteoblasts and osteoclasts. Moreover, testosterone and estrogen may affect osteoblasts differently at various skeletal locations (i.e. testosterone increases periosteal apposition of bone, whereas estrogen opposes it). This results in larger skeleton achieved by males than females during puberty.

If prolonged estrogen stimulation in the premenopausal period contributes to development of HFI (7, 13), we can expect estrogen to have an impact in other skeletal

sites as well. To test this hypothesis, we analyzed densitometric parameters in two other regions: vertebral spine and hip region. Women with HFI tended to have increased values of densitometric parameters in all the investigated regions, but without significant differences when compared to the age-matched post-menopausal control group. This trend was also present when comparing moderate HFI and severe HFI to the control group, i.e. women with the severe form of HFI had the highest values of BMD in neck, total hip and vertebral region, compared to those with moderate HFI and women without HFI, although the differences were not statistically significant.

More pronounced external morphological traits of the skull have been described in women with HFI (7, 42). Having in mind that size of brow ridge and external occipital protuberance are the most sexually dimorphic characteristics of the skull and that they are more pronounced in males (79), these results may suggest that with advancing manifestation of HFI, skulls of these women become more “male like”. We tried to determine whether similar external morphological changes were present in other skeletal sites, such as the femur. Comparison of the length, periosteal diameter and cortical thickness of femoral neck, intertrochanteric region and femoral shaft, between women with HFI and the age-matched control group did not indicate any significant differences. The results of our study suggest that new bone formation in women with HFI is localized only on the skull, unlike the results of Kollin and Fehér (19) who implied generalized nature of this condition.

In the “global model” of HFI pathogenesis proposed by Hershkovitz et al. (7), authors have suggested that neovascularization originating from dura might be one of the key processes in development of HFI. The cranial dura mater is a fibrous membrane, consisted of two layers, endosteal and meningeal, separated by lacunar spaces and blood vessels. Endosteal layer serves as the internal periosteum for the cranial bones, and contains the blood vessels for their supply while meningeal layer is consisted of mesothelium (38). Both frontal bone and its underlying dura mater originate from cephalic neural crest cells (40, 80). This embryogenic intimacy of the frontal bone and its underlying dura could be important in clarifying the development of HFI.

Levine et al. (1998) showed that the dura mater differs in different regions of cranial vault (81). During research of the suture closure in experimental rats, they

rotated dura mater underlying patient and fusing sutures and detected that dura is responsible for osteogenic signals that are controlling suture fusion. This mechanism is important since fetal and infant dura mater is highly osteogenic and capable of completely re-ossifying the cranial vault (82). Yu et al. (1997) suggested that dura mater is capable of inducing bone formation in general (83) by activation of bone growth sites. Bone growth sites are secondary, adaptive regions at which bone remodeling takes place. They remain dormant until stimulated to make bone by some external signal. In the cranial vault, the stimulus arises primarily from the expanding brain which is sending signals by means of the dura mater (84, 85).

The dura plays a role in intramembranous ossification of the skull vault in a regionally specific manner (86). Morphogenesis of the cranial bones is dependent on bone-tissue interactions with the dura matter, which controls the size and shape of these bones (87). Cells isolated from dura are multipotent in vitro, giving rise to many different cells, such as osteoblasts. This fact suggests the multipotent nature of dural cells in vivo (88). Dura stimulates osteoblast proliferation and it is the source of mitogenic growth factors (89). Therefore, the dura retains the ability to form bone tissue when cultured in vitro and implanted in vivo (88), supporting the speculation of its important role in HFI formation.

It is still unknown if sex steroid hormones influence the dura. Only a few studies have investigated this issue in animal models. Lin et al. (90) examined dural androgen receptors and suggested that sex steroid hormones may stimulate sutural osteogenesis by promoting osteodifferentiation of dural cells. Also, some studies investigated estrogen receptors (ER) and identified ER- α receptors on both calvaria and dura (86, 91). They found estrogen receptors localized mostly on the vascular tissue of dura and suggested that estrogen plays an important role in meningeal vascularity (91). This fact might explain specific vascularization running from the dura into the bone, which is proposed in the global model of HFI pathogenesis. Although dural estrogen-responsive cells are recognized, no explanation exists about the source of estrogen and whether it is regional or distant. Some researchers have suggested that the dura, as a source of paracrine factors important for suture fusion, could also be a source of regional estrogen production (86). Having in mind the regional differentiation of cranial dura (86), it can

be speculated that the frontal bone is particularly affected by HFI due to specific properties of its underlying dura.

In an attempt to test this speculation and the possible role of estrogen in pathogenesis of HFI, we tried to investigate the expression of α -estrogen receptors on dura of the frontal region in women with HFI and age-matched control group. Unfortunately, our results were poor since positivity for α -estrogen receptors on dura of the frontal region was present in just three of all investigated cases. These negative results could bring into question the role of estrogen in the development of HFI. However, they can imply that the receptors for estrogen are localized on the bone instead of dura, but due to hypo-cellularity of the frontal bone samples in women with HFI, it is difficult to detect and quantify them. Also, the question imposes whether the number of estrogen receptors on dura is positively correlated to the concentration of circulating estrogen (92) or circulating estrogen causes their down regulation, thus whether our results support increased or decreased estrogen stimulation.

Additionally, previous studies focusing on HFI provided limited insights into the pathogenesis of this phenomenon. Current macroscopic classification defines four grades/stages of HFI based on the morphological appearance and size of the affected area; however, it remains unclear whether different macroscopic stages of HFI can be regarded as successive phases in the process of HFI development. Hence, we assessed microarchitecture of the frontal bone in women with various types of HFI expression and in an age- and sex-matched control group, hypothesizing that bone microarchitecture bears imprints of the pathogenesis of *hyperostosis frontalis interna* and may clarify the phases of its development.

Although it could be expected that HFI ultimately leads to bone sclerosis, our microstructural analysis of the whole bone thickness showed no significant differences in the total bone volume fraction between the frontal bone samples from HFI at any stage and control groups. However, micro-CT evaluation of the bone samples showed a different pattern of bone microarchitectural organization in women with HFI when compared to age- and sex-matched control group. Specifically, the samples with HFI displayed more porous inner table of the frontal bone, while the diploic space showed an increased bone volume fraction due to thicker and more plate-like trabeculae.

”Global model” of HFI proposed by Hershkovitz et al. (7) considers vascularization originating from the dura as one of the key factors in pathogenesis of HFI. Talarico et al. (68) reported that in the woman with HFI inner table exhibited extensive remodeling, consisted almost exclusively of large sinuses and extended to the external periosteal layer of the dura. Our findings of significantly higher porosity of the inner table in women with HFI compared to controls may suggest increased penetration of dural vessels to the inner table. Furthermore, in women with HFI a significantly higher porosity was evident in the inner table compared to the outer table. Analysis of the distribution of pore diameters between the outer and inner tables in women with HFI revealed that increased porosity of the inner table originates from more abundant pores larger than 100 μm . Considering that control group did not show such differences between inner and outer table it is likely that increased porosity of the inner table is related to the pathogenesis of HFI. Therefore, it is possible that larger pores occur as a result of penetration of blood vessels from the dura, ultimately leading to diploization of the inner table.

Although direct experimental evidence is still insufficient, it is likely that sex steroid hormones effects on development and proliferation of blood vessels may be involved. In general, estrogen receptors are localized mostly on the vascular tissue of dura and estrogen is known to play an important role in meningeal vascularity (91). Angiogenesis under estrogen stimulation has been widely investigated (93, 94). It has been suggested that estrogen activates hypoxia-inducible factor- α (HIF α) signaling pathway leading to activation of proangiogenic genes, primarily for vascular endothelial growth factor (VEGF) (94, 95). In this way estrogen can stimulate angiogenesis.

In order to test the possible relationship between sex steroid induced vascularization and development of HFI we analyzed changes in dural vascularity in women with HFI by investigating the expression of CD34 receptors on the dura of the frontal region in women with HFI and the control group. Our result showed that in women with HFI expression of CD34 was significantly higher, thus the vascularization was increased. These results clearly imply the correlation between the HFI formation and expanded blood supply of any origin. This way, we supported our results obtained by microstructural analyses which implied increased porosity in the region of inner table

in women with HFI as well as pathogenesis of HFI proposed by “global model”. The role of altered blood supply in the pathogenesis of HFI has a practical repercussion. It is important to determine whether osseous thickening or a shift in vascular structures in patients with HFI will lead to a change in the process of operational interventions in this anatomical region as these bone overgrowths are close to the brain tissue (96).

There is also multiple evidence that bone turnover is related to bone vasculature (97-99). In particular, blood vessels’ endothelium may be a key factor in such a relationship, being not only an essential barrier limiting the movement of cells and molecules between the circulation and bone surface but also able to directly communicate with adjacent tissue and circulating blood cells (97). Endothelial cells (EC) are capable of responding to bone modulators (such as sex steroid hormones) and can release regulatory molecules (growth factors, BMPs, cytokines, endothelins, free radicals, prostanoids) known to affect the differentiation, metabolism, survival, and function of bone forming cells (97, 100). As EC also separate mesenchymal stem cells (MSC) in peripheral circulation from the bone surface, MSC migration may be directly orchestrated by endothelial cells (101). Additionally, bone marrow stromal cells exhibit osteogenic potential under EC guidance (102).

Although the “global model” of HFI pathogenesis (7) suggests that diploic space is not directly involved in HFI, our microarchitectural findings demonstrated clear differences between HFI and control group in the diploe. Clearly, after blood vessels from the dura penetrate the inner table and enter the diploic space, they can branch extensively within the intertrabecular pores and, could modulate bone remodeling (96). Our micro-CT analysis showing thickened trabeculae and significantly increased bone volume fraction of the diploe in women with HFI compared to the control group clearly emphasized an osteogenic phenotype of the diploic region in women with HFI (Figure 21). Based on the molecular studies, increased osteogenesis can be accomplished by HIF α mediated estrogen modulation of EC functional interactions (increased migration of osteoblast precursors from circulation, increased production of VEGF, increased proliferation and differentiation of BMSC).

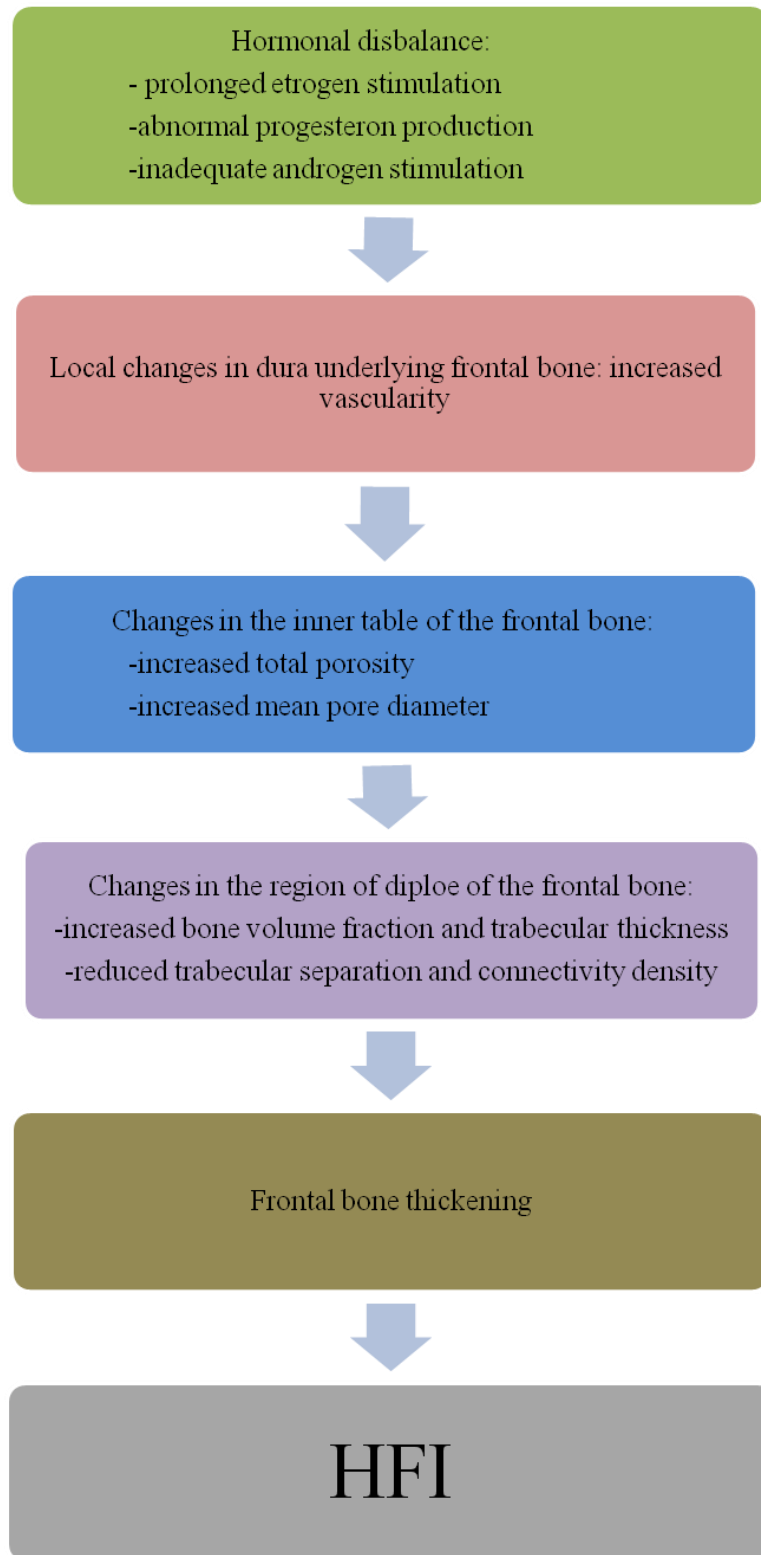


Figure 21. Schematic presentation of the changes in bone structure during HFI formation

Thus, the changes in bone microarchitecture in the region of diploe observed in our study (increase in BV/TV, trabecular thickness and microvascular density) could occur as a result of previously reported effects of activated HIF- α signaling pathway (95, 103). Previous studies in patients with HFI also demonstrated similar trend of altered bone structure in the region of diploe such as trabecular thickening (104) and sclerotic and dense internal part of diploe with small cavities in the final phase of HFI formation (105). Common macroscopic classification of HFI describes four types of this phenomenon (A, B, C and D) that are often regarded as “phases” or consecutive “stages” in the course of HFI development. However, our study showed that these macroscopic phases could not be distinguished at the level of bone microarchitecture and their consecutive nature cannot be further supported. Specifically, the comparisons of types A, B, C and D of HFI and control group suggested that significant inter-group differences in microstructural parameters existed only between the type D of HFI and control group. Therefore, based on our microarchitectural evaluation of macroscopic stages of HFI we can suggest that only two different types of HFI should be considered: moderate (comprising the types A, B and C) and severe HFI (comprising type D). Macroscopic grades of HFI could not be distinguished at the level of bone microarchitecture and their consecutive nature cannot be supported. Rather, our study suggests that only two different types of HFI (moderate and severe HFI) have microstructural justification and should be further considered. It is essential to record HFI systematically in human postmortem subjects to provide more data on the mechanisms of its development.

Researchers have investigated the phenomenon of HFI in the context of its epidemiology, demographics and possible relation to different conditions (16, 51-53, 55, 67, 106). Despite this fact, there is a limited data providing adequate classification of this variable change in the frontal bone thickness and morphology, practical for routine radiological and clinical practice. Therefore, successful radiological identification of HFI is relatively low. Predominantly, low percentage of recognition occur in cases of mild forms of HFI, while in more severe cases recognition of HFI is much more successful, even in standard radiographs (7). Having in mind variety of condition and disorders that might be related to HFI, systematic recording of HFI in medical records

can be helpful in distinguishing whether reported disorders occur as a consequence of HFI or are related to other diseases.

Present, widely accepted, macroscopical classification of HFI, proposed by Hershkovitz et al. (7), recognises four different types of HFI (A, B, C and D) based on extent of involvement of the frontal bone, appearance, border type, shape, location in frontal bone and involvement of other bones. The same research group who proposed this classification of HFI, tended to simplify it throughout different research, by regrouping HFI in fewer categories. When May et al. (107) investigated HFI in a context of sexing and aging a skeleton, they modified the present classification, and defined two types of HFI: minor HFI (equivalent to type B) and major HFI (equivalent to types C and D) while when they investigated intracranial volume and cranial thickness in elderly patients with HFI (71), they merged type A of HFI and patients without HFI, while types B, C and D remained as previously described. Therefore, we recognized the need to simplify the current classification of HFI and test it in order to standardize the classification method and to eliminate the observer's subjectivity.

Thickening of the frontal bone described as HFI, results in irregularity of the shape of the inner table of the frontal bone, and consequently the inner table of the skull. Irregular shapes are difficult to analyze and compare. In order to compare them objectively we need to quantify them. In this study, we used the mathematical method of fractal analyses, which allowed us to compare the irregular shapes of the inner table of the skull (inner contour) in women with different types of HFI. The irregularity of the shape of the inner contour of the skull was quantified using the values of fractal dimension and the circularity. By comparing these descriptive parameters, we tested current classification of HFI.

The fractal dimension is a geometrical parameter, which describes irregularly shaped objects (108). Our results reported no differences in fractal dimension values between different types of HFI. However, having the same fractal dimension doesn't exclude that that two objects may appear morphologically very different from each other (109) and these results might occur due to the fact that two samples showing the same fractal dimension could have different morphological patterns (i.e. different types of HFI). Circularity is commonly used as a parameter which quantifies the shape of 2-

dimensional objects (64). Our results reported significant differences in values of this parameter, between the type D and types A, B and C of HFI. These results suggest that types A, B and C of HFI should be considered as one type (mild HFI) while type D of HFI should remain separated (severe HFI). Our findings suggest that circularity could be considered an adequate parameter of shape of inner contour of the skull in patients with different types of HFI. Finally, the classification of HFI obtained by method of fractal analysis demonstrated the same results reported during microstructural analysis of bone samples from women with HFI, where significant differences in microarchitectural parameters were detected only between type D of HFI in comparison to types A, B and C of HFI. Reported results imply that HFI should be reclassified into two different types: moderate and severe.

6 Conclusions

1. HFI is associated with higher prevalence of headache, neurological and psychiatric disorders and a significantly lower prevalence of having given birth.
2. Apart from thicker frontal bone, women with HFI have thicker occipital and parietal bones as well. Frontal bone is the first one to thicken, followed by parietal and occipital bones respectively.
3. New bone formation and altered external morphology in women with HFI are localized only on the skull, while DXA results showed that with the increase of HFI magnitude, there is a tendency of increased bone density in the region of hip and spine, but without statistical significance.
4. Negative results of estrogen receptors analysis on the dura underlying frontal bone still do not exclude the effects of estrogen in the development of HFI.
5. Vascularization of the dura underlying frontal bone of women with HFI is increased implying the correlation between the HFI formation and expanded blood supply of any origin.
6. Inner table of the frontal bone in women with HFI shows higher porosity originating from more abundant pores larger than 100 μm possibly as a result of penetration of blood vessels from the dura.
7. Women with HFI showed microstructural differences in the region of diploe of the frontal bone. Thickened trabeculae and significantly increased bone volume fraction clearly emphasize an osteogenic phenotype of the diploic region in women with HFI, while outer table remains unchanged.
8. Macroscopic types of HFI could not be distinguished at the level of bone microarchitecture and their consecutive nature cannot be supported. Rather, our study suggests that only two different types of HFI (moderate and severe HFI) have microstructural justification and should be further considered.

9. Results of analysis of the parameters of shape of inner contour of the skull and microstructural analysis of the frontal bone samples both implied that HFI should be reclassified into two different types: moderate and severe. This way we also simplified the method of radiological classification of HFI.

7 References

1. Morgagni GB. *Adversaria anatomica VI. Animadversio LXXIV.* Padua: Vulporius; 1719.
2. Stewart R. Localized cranial hyperostosis in the insane. *J Neurol Psychopathol.* 1928(8):321–31.
3. Morel F. Hyperostosis frontalis interna and cerebral symptoms. *Confin Neurol.* 1951;11(1):9-13.
4. Moore S. *Hyperostosis cranii.* Springfield, IL: Charles C. Thomas; 1955.
5. Anton SC. Endocranial hyperostosis in Sangiran 2, Gibraltar 1, and Shanidar 5. *Am J Phys Anthropol.* 1997;102(1):111-22.
6. Perou M. *Cranial hyperostosis.* Springfield, IL: Charles C. Thomas; 1964.
7. Hershkovitz I, Greenwald C, Rothschild BM, Latimer B, Dutour O, Jellema LM, et al. Hyperostosis frontalis interna: an anthropological perspective. *Am J Phys Anthropol.* 1999;109(3):303-25.
8. D Resnick GN. *Diagnosis of bone and joint disorders.* Philadelphia: Saunders; 1988.
9. Gershon-Cohen J, Schraer H, Blumberg N. Hyperostosis frontalis interna among the aged. *Am J Roentgenol Radium Ther Nucl Med.* 1955;73(3):396-7.
10. Marlet JJ. Development of cranial hyperostosis. A radiological approach to a process. *Radiologia clinica et biologica.* 1974;43(6):473-82.
11. Nikolic S, Djonic D, Zivkovic V, Babic D, Jukovic F, Djuric M. Rate of occurrence, gross appearance, and age relation of hyperostosis frontalis interna in females: a prospective autopsy study. *Am J Forensic Med Pathol.* 2010;31(3):205-7.
12. Raikos A, Paraskevas GK, Yusuf F, Kordali P, Meditskou S, Al-Haj A, et al. Etiopathogenesis of hyperostosis frontalis interna: a mystery still. *Ann Anat.* 2011;193(5):453-8.
13. Yamakawa K, Mizutani K, Takahashi M, Matsui M, Mezaki T. Hyperostosis frontalis interna associated with hypogonadism in an elderly man. *Age Ageing.* 2006;35(2):202-3.
14. Ramchandren S, Liebeskind DS. Headache in a patient with Klinefelter's syndrome and hyperostosis frontalis interna. *J Headache Pain.* 2007;8(6):342-4.

15. Salmi A, Voutilainen A, Holsti IR, Unnerus CE. Hyperostosis cranii in a normal population. *Am J Roentgenol Radium Ther Nucl Med.* 1962;87:1032-40.
16. Richter L. Zur Hyperostose des Stirnbeins. *Rontgenpraxis* 1939;11:651-62.
17. Calame MA. [Hyperostosis frontalis interna]. *Rev Med Suisse Romande.* 1951;71(11):748-50.
18. Morel F. L'hyperostose frontale interne. Syndrome de l'hyperostose frontale interne avec adiposite et troubles cerebraux. Paris: Doin; 1930.
19. Kollin E, Feher T. Androgens, bone mineral content and hyperostosis frontalis interna in pre-menopausal women. *Exp Clin Endocrinol.* 1986;87(2):211-4.
20. Musha Y. [Etiological study of spinal ligament ossification with special reference to dietary habits and serum sex hormones]. *Nihon Seikeigeka Gakkai zasshi.* 1990;64(11):1059-71.
21. Riggs BL, Khosla S, Melton LJ, 3rd. Sex steroids and the construction and conservation of the adult skeleton. *Endocrine reviews.* 2002;23(3):279-302.
22. May H, Peled N, Dar G, Abbas J, Medlej B, Masharawi Y, et al. Hyperostosis frontalis interna and androgen suppression. *Anat Rec (Hoboken).* 2010;293(8):1333-6.
23. Rudali G. Experimental production of hyperostosis frontalis interna in mice. *Isr J Med Sci.* 1968;4(6):1230-5.
24. Korenman SG. Oestrogen window hypothesis of the aetiology of breast cancer. *Lancet.* 1980;1(8170):700-1.
25. Ruhli FJ, Henneberg M. Are hyperostosis frontalis interna and leptin linked? a hypothetical approach about hormonal influence on human microevolution. *Med Hypotheses.* 2002;58(5):378-81.
26. Matkovic V, Ilich JZ, Skugor M, Badenhop NE, Goel P, Clairmont A, et al. Leptin is inversely related to age at menarche in human females. *J Clin Endocrinol Metab.* 1997;82(10):3239-45.
27. Watrous A.C. ASC, Plourde A., M. Hyperostosis frontalis interna in ancient Egyptians. *Am J Phys Anthropol.* 1993;16:205.
28. Hajdu T, Fothi E, Bernert Z, Molnar E, Lovasz G, Kovari I, et al. Appearance of hyperostosis frontalis interna in some osteoarcheological series from Hungary. *Homo.* 2009;60(3):185-205.

29. Mulhern DM, Wilczak CA, Dudar JC. Brief communication: unusual finding at Pueblo Bonito: multiple cases of hyperostosis frontalis interna. *Am J Phys Anthropol.* 2006;130(4):480-4.
30. Ruhli FJ, Boni T, Henneberg M. Hyperostosis frontalis interna: archaeological evidence of possible microevolution of human sex steroids? *Homo.* 2004;55(1-2):91-9.
31. Armelagos GJ, Chrisman OD. Hyperostosis frontalis interna: a Nubian case. *Am J Phys Anthropol.* 1988;76(1):25-8.
32. May H, Peled N, Dar G, Abbas J, Hershkovitz I. Hyperostosis frontalis interna: what does it tell us about our health? *Am J Hum Biol.* 2011;23(3):392-7.
33. Strassmann BI. Menstrual cycling and breast cancer: an evolutionary perspective. *Journal of women's health / the official publication of the Society for the Advancement of Women's Health Research.* 1999;8(2):193-202.
34. Gerstman BB, Gross TP, Kennedy DL, Bennett RC, Tomita DK, Stadel BV. Trends in the content and use of oral contraceptives in the United States, 1964-88. *American journal of public health.* 1991;81(1):90-6.
35. Stefanick ML. Estrogens and progestins: background and history, trends in use, and guidelines and regimens approved by the US Food and Drug Administration. *The American journal of medicine.* 2005;118 Suppl 12B:64-73.
36. Andersson AM, Skakkebaek NE. Exposure to exogenous estrogens in food: possible impact on human development and health. *European journal of endocrinology / European Federation of Endocrine Societies.* 1999;140(6):477-85.
37. Cassidy A, Faughnan M. Phyto-oestrogens through the life cycle. *The Proceedings of the Nutrition Society.* 2000;59(3):489-96.
38. Gray H. *Anatomy of the human body.* Philadelphia: Lea & Febiger; 1918.
39. Chai Y, Ito Y, Han J. TGF-beta signaling and its functional significance in regulating the fate of cranial neural crest cells. *Critical reviews in oral biology and medicine : an official publication of the American Association of Oral Biologists.* 2003;14(2):78-88.
40. Couly GF, Coltey PM, Le Douarin NM. The triple origin of skull in higher vertebrates: a study in quail-chick chimeras. *Development (Cambridge, England).* 1993;117(2):409-29.

41. Jiang X, Iseki S, Maxson RE, Sucov HM, Morriss-Kay GM. Tissue origins and interactions in the mammalian skull vault. *Developmental biology*. 2002;241(1):106-16.
42. May H, Mali Y, Dar G, Abbas J, HersHKovitz I, Peled N. Intracranial volume, cranial thickness, and hyperostosis frontalis interna in the elderly. *Am J Hum Biol*. 2012;24(6):812-9.
43. Barber G, Watt I, Rogers J. A comparison of radiological and palaeopathological diagnostic criteria for hyperostosis frontalis interna. *Int J Osteoarchaeol*. 1997;7:157-64.
44. Takeuchi Y, Matsumoto T, Takuwa Y, Hoshino Y, Kurokawa T, Shibuya N, Ogat, E. High incidence of obesity and elevated serum immunoreactive insulin level in patients with paravertebral ligamentous ossification: a relationship to the development of ectopic ossification. *Journal of bone and mineral metabolism*. 1989;50:17-21.
45. Verdy M, Guimond J, Fauteux P, Aube M. Prevalence of hyperostosis frontalis interna in relation to body weight. *Am J Clin Nutr*. 1978;31(11):2002-4.
46. Dann S. Metabolic craniopathy: a review of the literature with report of a case with diabetes insipidus. *Ann Intern Med*. 1951;34(1):163-202.
47. Verdy M, Fauteux P, Caron D. Letter: Hyperostosis frontalis interna and serum enzymes in obese women. *Ann Intern Med*. 1974;81(3):409-11.
48. Verdy M, Levesque HP, Boghen D, Aube M, Guimond J. Manual dexterity test in relation to obesity and hyperostosis frontalis interna in elderly women. *Gerontology*. 1980;26(1):50-2.
49. Lahlou N, Landais P, De Boissieu D, Bougneres PF. Circulating leptin in normal children and during the dynamic phase of juvenile obesity: relation to body fatness, energy metabolism, caloric intake, and sexual dimorphism. *Diabetes*. 1997;46(6):989-93.
50. Pawlikowski M, Komorowski J. Hyperostosis frontalis, galactorrhoea/hyperprolactinaemia, and Morgagni-Stewart-Morel syndrome. *Lancet*. 1983;1(8322):474.
51. Pawlikowski M, Komorowski JM. Hyperostosis frontalis and prolactin secretion. *Exp Clin Endocrinol*. 1987;89(1):109-11.
52. Fulton JD, Shand J, Ritchie D, McGhee J. Hyperostosis frontalis interna, acromegaly and hyperprolactinaemia. *Postgrad Med J*. 1990;66(771):16-9.

53. Attanasio F, Granziera S, Giantin V, Manzato E. Full penetrance of Morgagni-Stewart-Morel syndrome in a 75-year-old woman: case report and review of the literature. *J Clin Endocrinol Metab.* 2013;98(2):453-7.
54. Devriendt W, Piercecchi-Marti MD, Adalian P, Sanvoisin A, Dutour O, Leonetti G. Hyperostosis frontalis interna: forensic issues. *J Forensic Sci.* 2005;50(1):143-6.
55. Cetiner Batun G, Yuruyen M, Vatankulu B, Elmali AD, Emul M. Hyperostosis frontalis interna presenting as depression and parkinsonism in an older woman. *Psychogeriatrics.* 2015.
56. Ntlholang O, Mahon O, Bradley D, Harbison JA. Does hyperostosis frontalis interna have any clinical relevance in stroke patients? *QJM.* 2014;107(9):783-4.
57. Walinder J. Hyperostosis frontalis interna and mental morbidity. *Br J Psychiatry.* 1977;131:155-9.
58. Thevoz F. The dura mater and its vessels in the morphogenesis of hyperostosis frontalis interna. *Ann Anat Pathol (Paris).* 1966;11(2):121-49.
59. Landis JR, Koch GG. An application of hierarchical kappa-type statistics in the assessment of majority agreement among multiple observers. *Biometrics.* 1977;33(2):363-74.
60. Djonc D, Milovanovic P, Nikolic S, Ivovic M, Marinkovic J, Beck T, et al. Inter-sex differences in structural properties of aging femora: implications on differential bone fragility: a cadaver study. *Journal of bone and mineral metabolism.* 2011;29(4):449-57.
61. Vermeulen PB, Gasparini G, Fox SB, Toi M, Martin L, McCulloch P, et al. Quantification of angiogenesis in solid human tumours: an international consensus on the methodology and criteria of evaluation. *European journal of cancer (Oxford, England: 1990).* 1996;32a(14):2474-84.
62. Milosevic NT, Ristanovic D, Maric DL, Rajkovic K. Morphology and cell classification of large neurons in the adult human dentate nucleus: a quantitative study. *Neuroscience letters.* 2010;468(1):59-63.
63. Ristanovic D, Milosevic NT, Stefanovic BD, Maric DL, Rajkovic K. Morphology and classification of large neurons in the adult human dentate nucleus: a qualitative and quantitative analysis of 2D images. *Neuroscience research.* 2010;67(1):1-7.

64. Milosevic NT, Ristanovic D, Jelinek HF, Rajkovic K. Quantitative analysis of dendritic morphology of the alpha and delta retinal ganglion cells in the rat: a cell classification study. *Journal of theoretical biology*. 2009;259(1):142-50.
65. Culafic D, Djonic D, Culafic-Vojinovic V, Ignjatovic S, Soldatovic I, Vasic J, et al. Evidence of degraded BMD and geometry at the proximal femora in male patients with alcoholic liver cirrhosis. *Osteoporosis international : a journal established as result of cooperation between the European Foundation for Osteoporosis and the National Osteoporosis Foundation of the USA*. 2015;26(1):253-9.
66. Kocabas H, Sezer I, Melikoglu MA, Gurbuz U, Illeez O, Ozbudak IH, et al. Hyperostosis frontalis interna in a patient with giant cell arteritis. *Mod Rheumatol*. 2008;18(2):181-3.
67. Chaljub G, Johnson RF, 3rd, Johnson RF, Jr., Sitton CW. Unusually exuberant hyperostosis frontalis interna: MRI. *Neuroradiology*. 1999;41(1):44-5.
68. Talarico EF, Prather AD, Hardt KD. A case of extensive hyperostosis frontalis interna in an 87-year-old female human cadaver. *Clin Anat*. 2008;21(3):259-68.
69. Hasegawa T, Ito H, Yamamoto S, Haba K, Murata H. Unilateral hyperostosis frontalis interna. Case report. *J Neurosurg*. 1983;59(4):710-3.
70. Charleston L 4th, Strabbing R, Cooper W. Is sinus disease the cause of my headaches? An update on sinus disease and headache. *Current pain and headache reports*. 2014;18(6):418.
71. May H, Peled N, Dar G, Hay O, Abbas J, Masharawi Y, et al. Identifying and classifying hyperostosis frontalis interna via computerized tomography. *Anat Rec (Hoboken)*. 2010;293(12):2007-11.
72. Andreasen NC, Flaum M, Swayze V, 2nd, O'Leary DS, Alliger R, Cohen G, et al. Intelligence and brain structure in normal individuals. *The American journal of psychiatry*. 1993;150(1):130-4.
73. Hughes DE, Dai A, Tiffée JC, Li HH, Mundy GR, Boyce BF. Estrogen promotes apoptosis of murine osteoclasts mediated by TGF-beta. *Nature medicine*. 1996;2(10):1132-6.
74. Manolagas SC. Birth and death of bone cells: basic regulatory mechanisms and implications for the pathogenesis and treatment of osteoporosis. *Endocrine reviews*. 2000;21(2):115-37.

75. Kuiper GG, Enmark E, Peltö-Huikko M, Nilsson S, Gustafsson JA. Cloning of a novel receptor expressed in rat prostate and ovary. *Proceedings of the National Academy of Sciences of the United States of America*. 1996;93(12):5925-30.
76. Pettersson K, Grandien K, Kuiper GG, Gustafsson JA. Mouse estrogen receptor beta forms estrogen response element-binding heterodimers with estrogen receptor alpha. *Molecular endocrinology (Baltimore, Md)*. 1997;11(10):1486-96.
77. Arts J, Kuiper GG, Janssen JM, Gustafsson JA, Lowik CW, Pols HA, et al. Differential expression of estrogen receptors alpha and beta mRNA during differentiation of human osteoblast SV-HFO cells. *Endocrinology*. 1997;138(11):5067-70.
78. Falahati-Nini A, Riggs BL, Atkinson EJ, O'Fallon WM, Eastell R, Khosla S. Relative contributions of testosterone and estrogen in regulating bone resorption and formation in normal elderly men. *The Journal of clinical investigation*. 2000;106(12):1553-60.
79. W. B. Human osteology: a laboratory and field method. Springfield, IL: Charles C. Thomas; 1995.
80. Couly GF, Coltey PM, Le Douarin NM. The developmental fate of the cephalic mesoderm in quail-chick chimeras. *Development (Cambridge, England)*. 1992;114(1):1-15.
81. Levine JP, Bradley JP, Roth DA, McCarthy JG, Longaker MT. Studies in cranial suture biology: regional dura mater determines overlying suture biology. *Plastic and reconstructive surgery*. 1998;101(6):1441-7.
82. Hobar PC, Schreiber JS, McCarthy JG, Thomas PA. The role of the dura in cranial bone regeneration in the immature animal. *Plastic and reconstructive surgery*. 1993;92(3):405-10.
83. Yu JC, McClintock JS, Gannon F, Gao XX, Mobasser JP, Sharawy M. Regional differences of dura osteoinduction: squamous dura induces osteogenesis, sutural dura induces chondrogenesis and osteogenesis. *Plastic and reconstructive surgery*. 1997;100(1):23-31.
84. Baer MJ. Patterns of growth of the skull as revealed by vital staining. *Human biology*. 1954;26(2):80-126.

85. Moss ML. Growth of the calvaria in the rat; the determination of osseous morphology. *The American journal of anatomy*. 1954;94(3):333-61.
86. James AW, Theologis AA, Brugmann SA, Xu Y, Carre AL, Leucht P, et al. Estrogen/estrogen receptor alpha signaling in mouse posterofrontal cranial suture fusion. *PLoS One*. 2009;4(9):e7120.
87. Slater BJ, Kwan MD, Gupta DM, Amasha RR, Wan DC, Longaker MT. Dissecting the influence of regional dura mater on cranial suture biology. *Plastic and reconstructive surgery*. 2008;122(1):77-84.
88. Gagan JR, Tholpady SS, Ogle RC. Cellular dynamics and tissue interactions of the dura mater during head development. *Birth defects research Part C, Embryo today : reviews*. 2007;81(4):297-304.
89. White AP, Vaccaro AR, Hall JA, Whang PG, Friel BC, McKee MD. Clinical applications of BMP-7/OP-1 in fractures, nonunions and spinal fusion. *International orthopaedics*. 2007;31(6):735-41.
90. Lin IC, Slemper AE, Hwang C, Sena-Esteves M, Nah HD, Kirschner RE. Dihydrotestosterone stimulates proliferation and differentiation of fetal calvarial osteoblasts and dural cells and induces cranial suture fusion. *Plastic and reconstructive surgery*. 2007;120(5):1137-47.
91. Glinskii OV, Abraha TW, Turk JR, Rubin LJ, Huxley VH, Glinsky VV. Microvascular network remodeling in dura mater of ovariectomized pigs: role for angiotensin-1 in estrogen-dependent control of vascular stability. *Am J Physiol Heart Circ Physiol*. 2007;293(2):H1131-7.
92. Classen-Linke I, Alfer J, Hey S, Krusche CA, Kusche M, Beier HM. Marker molecules of human endometrial differentiation can be hormonally regulated under in-vitro conditions as in-vivo. *Hum Reprod Update*. 1998;4(5):539-549.
93. Liu LH, Lai Y, Linghu LJ, Liu YF, Zhang Y. Effect of different concentrations of medroxy-progesterone acetate combined with 17beta-estradiol on endothelial progenitor cells. *European review for medical and pharmacological sciences*. 2015;19(10):1790-5.
94. Yun SP, Lee MY, Ryu JM, Song CH, Han HJ. Role of HIF-1alpha and VEGF in human mesenchymal stem cell proliferation by 17beta-estradiol: involvement of PKC,

- PI3K/Akt, and MAPKs. *American journal of physiology Cell physiology*. 2009;296(2):C317-26.
95. Peng J, Lai ZG, Fang ZL, Xing S, Hui K, Hao C, et al. Dimethyloxalylglycine prevents bone loss in ovariectomized C57BL/6J mice through enhanced angiogenesis and osteogenesis. *PLoS One*. 2014;9(11):e112744.
96. Govsa F, Ozer MA, Pinar Y, Sezak M. Increased osseous thickening of the inner surface of the frontal bone. *Turk Neurosurg*. 2015;25(2):224-30.
97. Brandi ML, Collin-Osdoby P. Vascular biology and the skeleton. *Journal of bone and mineral research : the official journal of the American Society for Bone and Mineral Research*. 2006;21(2):183-92.
98. Pufe T, Claassen H, Scholz-Ahrens KE, Varoga D, Drescher W, Franke AT, et al. Influence of estradiol on vascular endothelial growth factor expression in bone: a study in Gottingen miniature pigs and human osteoblasts. *Calcified tissue international*. 2007;80(3):184-91.
99. Griffith JF, Wang YX, Zhou H, Kwong WH, Wong WT, Sun YL, et al. Reduced bone perfusion in osteoporosis: likely causes in an ovariectomy rat model. *Radiology*. 2010;254(3):739-46.
100. Streeten EA, Ornberg R, Curcio F, Sakaguchi K, Marx S, Aurbach GD, et al. Cloned endothelial cells from fetal bovine bone. *Proceedings of the National Academy of Sciences of the United States of America*. 1989;86(3):916-20.
101. Imai K, Kobayashi M, Wang J, Shinobu N, Yoshida H, Hamada J, et al. Selective secretion of chemoattractants for haemopoietic progenitor cells by bone marrow endothelial cells: a possible role in homing of haemopoietic progenitor cells to bone marrow. *British journal of haematology*. 1999;106(4):905-11.
102. von Schroeder HP, Veillette CJ, Payandeh J, Qureshi A, Heersche JN. Endothelin-1 promotes osteoprogenitor proliferation and differentiation in fetal rat calvarial cell cultures. *Bone*. 2003;33(4):673-84.
103. Weng T, Xie Y, Huang J, Luo F, Yi L, He Q, et al. Inactivation of Vhl in osteochondral progenitor cells causes high bone mass phenotype and protects against age-related bone loss in adult mice. *Journal of bone and mineral research: the official journal of the American Society for Bone and Mineral Research*. 2014;29(4):820-9.

104. She R, Szakacs J. Hyperostosis frontalis interna: case report and review of literature. *Ann Clin Lab Sci*. 2004;34(2):206-8.
105. Ruhli FJ, Kuhn G, Evison R, Muller R, Schultz M. Diagnostic value of micro-CT in comparison with histology in the qualitative assessment of historical human skull bone pathologies. *Am J Phys Anthropol*. 2007;133(4):1099-111.
106. Glab H, Szostek K, Kaczanowski K. Hyperostosis frontalis interna, a genetic disease?: Two medieval cases from Southern Poland. *Homo*. 2006;57(1):19-27.
107. May H, Peled N, Dar G, Cohen H, Abbas J, Medlej B, et al. Hyperostosis frontalis interna: criteria for sexing and aging a skeleton. *Int J Legal Med*. 2011;125(5):669-73.
108. Di Ieva A, Grizzi F, Sherif C, Matula C, Tschabitscher M. Angioarchitectural heterogeneity in human glioblastoma multiforme: a fractal-based histopathological assessment. *Microvascular research*. 2011;81(2):222-30.
109. Milosevic NT, Ristanovic D, Gudovic R, Rajkovic K, Maric D. Application of fractal analysis to neuronal dendritic arborisation patterns of the monkey dentate nucleus. *Neuroscience letters*. 2007;425(1):23-7.

Др Ђурђа Брацановић рођена је 1. јуна 1984. године у Београду. Основну школу „Сава Ковачевић“ завршила је 1999. године, а 2003. године и V београдску гимназију (природно-математички смер). На Медицински факултет у Београду уписала се 2003. године. Дипломирала је 2009. године са просечном оценом 9,07 (девет, нула седам). Докторске студије – смер Биологија скелета (на енглеском језику) уписала је 2009. године на Медицинском факултету у Београду. Од 2007. године је члан истраживачког тима Лабораторије за антропологију Института за анатомију Медицинског факултета у Београду, којом руководи проф. др Марија Ђурић. Од 2011. године ради као сарадник на пројекту III45005 који финансира Министарство просвете и науке Републике Србије. Аутор је или коаутор 4 рада штампаних у целини у часописима индексираним у JCR листи. У мају 2012. године, изабрана је у звање асистента на предмету Основи клиничке радиологије на Стоматолошком факултету Универзитета у Београду. Специјализацију из Радиологије на Медицинском факултету у Београду започела је 2012. године.

Prilog 1.

Izjava o autorstvu

Potpisana: Đurđa N. Bracanović

Broj upisa: 6/09

Izjavljujem

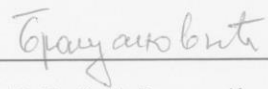
da je doktorska disertacija pod naslovom

„Radiološka i imunohistohemijska analiza hiperostoze frontalne kosti: multidisciplinarnan pristup u rasvetljavanju nastanka ovog fenomena“

- rezultat sopstvenog istraživačkog rada,
- da predložena disertacija u celini ni u delovima nije bila predložena za dobijanje bilo koje diplome prema studijskim programima drugih visokoškolskih ustanova,
- da su rezultati korektno navedeni i
- da nisam kršila autorska prava i koristila intelektualnu svojinu drugih lica.

Potpis doktoranda

U Beogradu, 30. maja 2016. godine



Dr Đurđa N. Bracanović

Prilog 2.

Izjava o istovetnosti štampane i elektronske verzije doktorskog rada

Ime i prezime autora: Đurđa N. Bracanović

Broj upisa: 6/09

Studijski program: Biologija skeleta

Naslov rada: „Radiološka i imunohistoheмиjska analiza hiperostoze frontalne kosti: multidisciplinarnan pristup u rasvetljavanju nastanka ovog fenomena“

Mentor: Doc. dr Danijela Đonić

Potpisana: Đurđa N. Bracanović

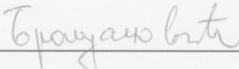
izjavljujem da je štampana verzija mog doktorskog rada istovetna elektronskoj verziji koju sam predala za objavljivanje na portalu **Digitalnog repozitorijuma Univerziteta u Beogradu**.

Dozvoljavam da se objave moji lični podaci vezani za dobijanje akademskog zvanja doktora nauka, kao što su ime i prezime, godina i mesto rođenja i datum odbrane rada.

Ovi lični podaci mogu se objaviti na mrežnim stranicama digitalne biblioteke, u elektronskom katalogu i u publikacijama Univerziteta u Beogradu.

Potpis doktoranda

U Beogradu, 30. maja 2016. godine



dr Đurđa N. Bracanović

Prilog 3.

Izjava o korišćenju

Ovlašćujem Univerzitetsku biblioteku „Svetozar Marković“ da u Digitalni repozitorijum Univerziteta u Beogradu unese moju doktorsku disertaciju pod naslovom:

„Radiološka i imunohistohemijska analiza hiperostoze frontalne kosti: multidisciplinarni pristup u rasvetljavanju nastanka ovog fenomena“

koja je moje autorsko delo.

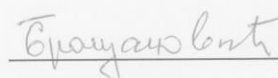
Disertaciju sa svim prilogima predala sam u elektronskom formatu pogodnom za trajno arhiviranje.

Moju doktorsku disertaciju pohranjenu u Digitalni repozitorijum Univerziteta u Beogradu mogu da koriste svi koji poštuju odredbe sadržane u odabranom tipu licence Kreativne zajednice (Creative Commons) za koju sam se odlučila.

1. Autorstvo
2. Autorstvo - nekomercijalno
3. Autorstvo – nekomercijalno – bez prerade
4. Autorstvo – nekomercijalno – deliti pod istim uslovima
5. Autorstvo – bez prerade
6. Autorstvo – deliti pod istim uslovima

Potpis doktoranda

U Beogradu, 30. maja 2016. godine



dr Đurđa N. Bracanović